You might find this additional info useful...

This article cites 62 articles, 12 of which you can access for free at:
http://jn.physiology.org/content/88/3/1097.full#ref-list-1

This article has been cited by 60 other HighWire-hosted articles:
http://jn.physiology.org/content/88/3/1097#cited-by

Updated information and services including high resolution figures, can be found at:
http://jn.physiology.org/content/88/3/1097.full

Additional material and information about *Journal of Neurophysiology* can be found at:
http://www.the-aps.org/publications/jn

This information is current as of May 28, 2013.

Sensorimotor Integration in Human Postural Control

R. J. PETERKA
Neurological Sciences Institute, Oregon Health & Science University, Portland, Oregon 97006

Peterka, R. J. Sensorimotor integration in human postural control. *J Neurophysiol* 88: 1097–1118, 2002; 10.1152/jn.00605.2001. It is generally accepted that human bipedal upright stance is achieved by feedback mechanisms that generate an appropriate corrective torque based on body-sway motion detected primarily by visual, vestibular, and proprioceptive sensory systems. Because orientation information from the various senses is not always available (eyes closed) or accurate (compliant support surface), the postural control system must somehow adjust to maintain stance in a wide variety of environmental conditions. This is the sensorimotor integration problem that we investigated by evoking anterior-posterior (AP) body sway using pseudorandom rotation of the visual surround and/or support surface (amplitudes 0.5–8°) in both normal subjects and subjects with severe bilateral vestibular loss (VL). AP rotation of body center-of-mass (COM) was measured in response to six conditions offering different combinations of available sensory information. Stimulus-response data were analyzed using spectral analysis to compute transfer functions and coherence functions over a frequency range from 0.017 to 2.23 Hz. Stimulus-response data were quite linear for any given condition and amplitude. However, overall behavior in normal subjects was nonlinear because gain decreased and phase functions sometimes changed with increasing stimulus amplitude. "Sensory channel reweighting" could account for this nonlinear behavior with subjects showing increasing reliance on vestibular cues as stimulus amplitudes increased. VL subjects could not perform this reweighting, and their stimulus-response behavior remained quite linear. Transfer function curve fits based on a simple feedback control model provided estimates of postural stiffness, damping, and feedback time delay. There were only small changes in these parameters with increasing visual stimulus amplitude. However, stiffness increased as much as 60% with increasing support surface amplitude. To maintain postural stability and avoid resonant behavior, an increase in stiffness should be accompanied by a corresponding increase in damping. Increased damping was achieved primarily by decreasing the apparent time delay of feedback control rather than by changing the damping coefficient (i.e., corrective torque related to body-sway velocity). In normal subjects, stiffness and damping were highly correlated with body mass and moment of inertia, with stiffness always about 1/3 larger than necessary to resist the destabilizing torque due to gravity. The stiffness parameter in some VL subjects was larger compared with normal subjects, suggesting that they may use increased stiffness to help compensate for their loss. Overall results show that the simple act of standing quietly depends on a remarkably complex sensorimotor control system.

INTRODUCTION

Bipedal upright stance is inherently unstable. A small sway deviation from a perfect upright position results in a torque due to gravity that accelerates the body further away from the upright position. To maintain upright stance, the destabilizing torque due to gravity must be countered by a corrective torque exerted by the feet against the support surface. A widely held view is that the corrective torque is generated through the action of a feedback control system (see reviews by Horak and Macpherson 1996; Johansson and Magnusson 1991). We will refer to this corrective torque, which necessarily involves a time delay due to sensory transduction, transmission, processing, and muscle activation, as "active" torque. However, controversy remains (Morasso and Schieppati 1999) because another view holds that the corrective torque is generated by muscle "tone" that acts without time delay (Winter et al. 1998, 2001). In this paper, we will refer to corrective torque that acts without time delay as "passive" torque. Finally, a third view recognizes that feedback mechanisms contribute to postural stabilization but states that feedback alone is insufficient and that feedforward predictive mechanisms are required to explain postural control behavior (Fitzpatrick et al. 1996). Our results support the view that active torque generated by feedback control mechanisms is the dominant contributor to quiet stance control.

Visual, proprioceptive, and vestibular systems clearly contribute to postural control because numerous studies have shown that stimulation of visual (Berthoz et al. 1979; Bronstein 1986; Dijkstra et al. 1994a; Lee and Lishman 1975; Lestienne et al. 1977; van Asten et al. 1988a), proprioceptive (Allum 1983; Jeka et al. 1997; Johansson et al. 1988; Kavounoudias et al. 1999), or vestibular systems (Day et al. 1997; Hlavacka and Nijiokiktjien 1985; Johansson et al. 1995; Nashner and Wolfson 1974) evoke body sway. However, little is known about how information from these senses is processed and combined to generate appropriate corrective torque when there is conflicting or inaccurate orientation information from different sensory systems. One possibility is that sensory cues are combined in an essentially linear manner. That is, each sensory system detects an "error" indicating deviation of body orientation from some reference position. Vestibular sensory cues detect deviations of head orientation from earth-vertical (gravity), visual sensors detect head orientation relative to the visual world, and proprioceptors detect leg orientation relative to the support surface. The individual error signals are summed, and appropriate corrective torque is generated as a function of this summed signal. Note that in this paper, for modeling purposes, we use a restricted definition of proprioceptive cues as only

Address for reprint requests: R. J. Peterka, Neurological Sciences Institute, OHSU West Campus, Bldg. 1, 505 NW 185th Ave., Beaverton, OR 97006 (E-mail: peterkar@ohsu.edu).

those sensory cues signaling body motion relative to the support surface. Additionally, we assume that appropriate neural transformations are performed on the various sensory cues so that the nervous system has information on body center-of-mass (COM) motion relative to each sensory reference (i.e., the direction of gravity for vestibular cues, visual world orientation for visual cues, and support surface orientation for proprioceptive cues). Psychophysical studies support the fact that such transformations can occur (Mergner et al. 1991, 1997).

Previous experimental results, where body sway was evoked by manipulation of individual and combined sensory cues, appear to be consistent with an essentially linear model (Fitzpatrick et al. 1996; Hajos and Kirchner 1984; Jeka et al. 1998, 2000; Johansson et al. 1988; Maki et al. 1987; Schöner 1991; van Asten et al. 1988b). Many of these earlier studies developed linear models that assumed that the postural control system was inherently stable, with experimental stimuli merely perturbing this inherently stable system. A more complete understanding of postural control must explain how this apparent inherent stability is actually achieved.

Most studies of human postural control have employed transient stimuli (e.g., sudden support surface motions) to evoke characteristic postural responses (Allum 1983; Diener et al. 1984b; Horak and Nashner 1986; Nashner 1977) or methods that artificially stimulate individual sensory receptors [i.e., muscle or tendon vibration (Kavounoudias et al. 1999) and galvanic vestibular stimulation (Nashner and Wolfson 1974; Watson and Colebatch 1997)]. We chose to investigate postural control using motion stimuli (tilts of the support surface and/or visual surround) that continuously perturb the system. Continuously varying stimuli (often sinusoidal stimuli over a range of frequencies, or more complex random or pseudorandom time series) evoke responses that eventually achieve a steady state. Steady-state stimulus-response data can be used to obtain transfer functions that characterize the dynamic properties of the system (Bendat and Piersol 2000). These techniques have been used previously to investigate postural control in humans and animals (Dijkstra et al. 1994b; Fitzpatrick et al. 1996; Hajos and Kirchner 1984; Ishida and Imai 1983; Jeka et al. 1998, 2000; Johansson et al. 1988; Maki et al. 1987; Peterka and Benolken 1995; Talbott 1980) but have not been systematically applied to investigate dynamic behavior over a wide range of conditions. The use of continuously applied perturbations seems appropriate to study quiet stance behavior, which itself is a continuously active process. This is in contrast to transient stimuli that may trigger specific and equally transient motor programs, which may not be directly related to the continuous regulation of balance.

Our results show that sensory integration and postural regulation do appear to be essentially linear processes for a specific sensory condition and a given stimulus amplitude. However, as stimulus conditions change, nonlinearities become apparent. The major nonlinearity occurs with changing stimulus amplitudes where there is an apparent graded shift in the source of sensory information contributing to postural control, with increasing utilization of vestibular cues as visual and proprioceptive perturbations increase. In subjects with absent vestibular function, this shift cannot occur, and their overall behavior remains quite linear independent of stimulus amplitude.

Such context-dependent changes in sensory utilization are in general agreement with previous views of postural behavior (Forssberg and Nashner 1982; Horak and Macpherson 1996; Nashner et al. 1982), experimental findings using galvanic vestibular stimulation (Britton et al. 1993; Fitzpatrick et al. 1994), and motor control in general (Hultborn 2001; Prochazka 1989). Our results provide quantitative measures of the stimulus-dependent changes in sensory contributions to postural control. In addition, our results provide estimates of important postural control parameters (stiffness, damping, time delay) and demonstrate how these parameters change in different sensory environments and stimulus conditions.

M E T H O D S

Subjects

The experimental protocols were approved by the Institutional Review Board at Oregon Health & Science University and were performed in accordance with the 1964 Helsinki Declaration. Prior to testing, all subjects gave their informed consent. Twelve subjects participated in this study. Eight were adults who had normal results on clinical sensory organization tests of postural control (Peterka and Black 1990) and had no known history of balance impairment or dizziness. The other four subjects had profound bilateral vestibular loss (VL subjects) as confirmed by clinical rotation testing and results from sensory organization tests of postural control (Nashner 1993a). The causes and durations of vestibular loss in these subjects are given in Table 1. Table 1 also shows the gain of horizontal vestibuloocular reflex (HVOR) for 0.05- and 0.2-Hz yaw rotations for the VL subjects. The HVOR gain for all VL subjects was well below the 95th percentile for the normal population (Peterka et al. 1990). The age range of normal subjects was 24–46 yr, while the VL subjects ranged in age from 45 to 58 yr. Although there was an age difference between these two groups, previous research has identified only minor changes in postural control in subjects in these age ranges (Peterka and Black 1990).

Experimental setup

All experiments were performed on a custom balance-testing device that included a motor-driven support surface and visual surround (Fig. 1). Position servo-controlled motors produced anterior/posterior (AP) tilts of the support surface and visual surround with the rotation axes collinear with the subject's ankle joints. Vertical force sensors in the support surface were used to measure center-of-pressure (COP) data. The visual surround had a half-cylinder shape (70-cm radius) and was lined with a complex checkerboard pattern consisting of white, black, and three gray levels (see Fig. 1). During testing, the room lights were off, and the visual surround was illuminated by fluorescent lights attached to the right and left edges of the surround.

During most experiments, the backboard assembly shown in Fig. 1

TABLE 1. *Vestibular loss subject demographics*

Subject	Age (years)	Duration of Loss (years)	Horizontal VOR Gain*		Cause of Loss
			0.05 Hz	0.2 Hz	
VL1	45	8	0.03	0.05	Viral
VL2	53	6	0.01	0.03	Viral
VL3	58	5	0.18	0.35	Gentamicin Ototoxicity
VL4	48	5	0.01	0.3	Gentamicin Ototoxicity

* Normal VOR gain range is 0.39–1.02 for 0.05 Hz and 0.40–1.02 for 0.2 Hz (Peterka et al. 1990).

FIG. 1. Balance test device. The subject stands on a support surface and views a high contrast visual surround. Both the support surface and visual surround can rotate in the anterior/posterior (AP) direction about the ankle joint axis. Single-link inverted pendulum dynamics are ensured by use of a backboard assembly. During freestanding trials, lightweight rods attached to potentiometers, located to the right and behind the subject, are used to measure AP body sway at hip and shoulder levels.

was used to constrain body motion to that of a single-link inverted pendulum with rotational motion occurring only in the AP direction. The subjects were secured to the backboard with a padded head rest and straps at the level of the subject's knees, hips, and shoulders. The backboard was attached at its base to a pair of bearings aligned with the subject's ankle joint axis. Therefore the subjects were not required to support the full weight of the backboard. However, the influence of backboard mass (12.6 kg) and moment of inertia (11.4 kg m^2) was accounted for in the data analysis. The body and backboard together acted as a single-link inverted pendulum. Body/backboard AP COM sway motion was provided by measures of backboard angular position, using a potentiometer, and angular velocity, using a rate sensor (Watson Industries, Eau Claire, WI). We considered these measures to be the output variables of interest.

During some experiments, the backboard assembly was not used and subjects were freestanding. In these experiments, AP body motion was measured by two horizontal rods attached to the subject at hip and shoulder levels (seen in Fig. 1, to the right of the subject). Rotational motion of the sway rods was recorded by potentiometers. Appropriate trigonometric conversions were made later to determine AP body displacement at hip and shoulder levels. A 120-s calibration trial was performed where subjects slowly leaned forward and backward using different combinations of leg and trunk rotations and minimizing knee flexion. A least-squared error curve fit of the following equation was used to obtain estimates of the coefficients a_h, a_s, and b

$$x_{cop}(t) = b + a_h x_h(t) + a_s x_s(t) \qquad (1)$$

where x_{cop} is AP COP displacement, x_h is AP body displacement at hip level, x_s is AP body displacement at shoulder level, and t is time. Because body movements were very slow, x_{cop} is essentially equal to AP COM displacement (except for small rapid oscillations about the local COM position indicative of AP body acceleration) (Brenière 1996; Winter et al. 1998). In subsequent trials, *Eq. 1* was used to calculate AP COM displacement from measures of $x_h(t)$ and $x_s(t)$. Then an estimate of the subject's COM height (based on anthropometric measures) above the ankle joint was used to calculate the COM rotation angle, which we considered to be the final output variable of interest.

Stimulus delivery and data sampling were computer controlled at a rate of 100/s. Sampled data included: visual surround and support surface angular position, four vertical forces from sensors at the corners of the support surface, rotational position of the hip and shoulder sway rods, and rotational position and velocity of the backboard assembly.

Pseudorandom stimuli

Rotational motion stimuli were based on a pseudorandom ternary sequence (PRTS) of numbers (Davies 1970). The method used to generate the pseudorandom stimulus waveforms is shown in Fig. 2. A stimulus was created from a 242-length PRTS sequence by assigning a rotational velocity waveform a fixed value of $+v$, 0, or $-v°$/s according to the PRTS sequence for a duration of $\Delta t = 0.25$ s (Fig. 2*B*, *top*). The duration of each stimulus cycle was 60.5 s. The mathematical integration of this PRTS velocity waveform gave a position waveform (Fig. 2*B*, *bottom*) that was delivered to the position servo motors to drive visual surround and/or support surface rotation. The PRTS stimulus has a wide spectral bandwidth (Fig. 2*C*) with the velocity waveform having spectral and statistical properties approximating a white noise stimulus (Davies 1970). As such, this stimulus appeared to be unpredictable to the test subject and thus likely limited any predictive contributions to postural responses that are known to occur (McIlroy and Maki 1994).

Protocol

The PRTS stimulus position waveform was scaled to provide five different stimulus amplitudes (0.5, 1, 2, 4, and 8° peak-to-peak). On most trials, six complete stimulus cycles were presented. On all 0.5° trials, and some 1° trials, eight cycles of the stimulus were presented. Table 2 provides a summary of all six test conditions. Appropriate control trials with duration equivalent to a six-cycle stimulus were also given. The starting value of the PRTS stimulus was selected so that about 80% of the rotational tilt occurred in the positive direction (i.e., toe down support surface tilt and visual surround tilt directed forward and away from the subject) because subjects are able to tolerate larger angle forward body tilts.
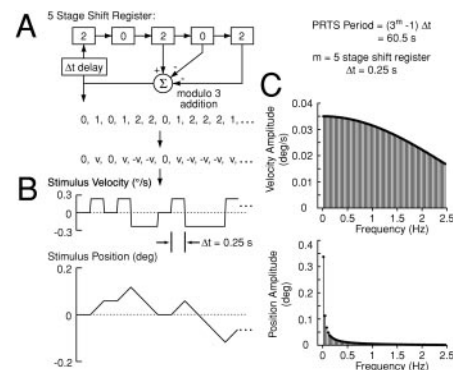

FIG. 2. Generation of a pseudorandom ternary sequence (PRTS) stimulus. *A*: a shift register with feedback is used to generate the PRTS. At each time increment, Δt, the value of each register is shifted to the right. A new value is entered into the left register based on modulo-3 addition of values in registers 3–5, and this new value is taken as the output. With the initial values shown in the 5 shift registers, the first 12 output values of the 242 value periodic sequence are shown below the shift register. This sequence is transformed into a velocity command sequence with values of $+v$, $-v$, or 0°/s. *B*: the velocity sequence is transformed into a velocity waveform by holding each velocity command for $\Delta t = 0.25$ s. The position waveform is the time integral of the velocity waveform. With $\Delta t = 0.25$ s, the PRTS waveform has a period of 60.5 s. *C*: the spectral composition of the complete velocity and position waveforms for a 1° peak-to-peak PRTS stimulus. Only odd-numbered spectral components have nonzero energy.

TABLE 2. *Description of test conditions and performance of vestibular loss subjects*

Test Condition	Visual Condition	Surface Condition	State of Sensory Information*			Number of VL Subjects Completing 1, 2, 4° PRTS Tests		
			Vision	Proprioception	Graviception	1°	2°	4°
1	PRTS Stimulus	Fixed	Accurate	Veridical	Veridical	4	4	4
2	PRTS Stimulus	Sway-referenced	Accurate	Inaccurate	Veridical	4	4	2
3	Fixed	PRTS Stimulus	Veridical	Accurate	Veridical	4	4	4
4	Eyes closed	PRTS Stimulus	Absent	Accurate	Veridical	4	4	3
5	Sway-referenced	PRTS Stimulus	Inaccurate	Accurate	Veridical	3	3	1
6	PRTS Stimulus	PRTS Stimulus	Accurate	Accurate	Veridical	4	4	4

* "Accurate" indicates that the sensory channel signal is time varying and providing accurate orientation information relative to the visual surround (vision) or support surface (proprioception), but is not providing veridical body-in-space orientation information. "Inaccurate" indicates that the sensory channel signal is not time varying and is not indicative of body orientation. VL, vestibular loss; PRTS, pseudorandom ternary sequence.

Two of the test conditions used "sway-referencing" of the support surface or visual surround to manipulate the orientation cues available for postural control (Nashner and Berthoz 1978). Sway-referencing was performed by commanding the support surface or visual surround servo systems to continuously track the subject's AP body-sway angle. When the backboard assembly was used, sway-referenced rotations of the visual surround or support surface tracked the rotational movement of the backboard. For freestanding trials, sway-referenced motions of the support surface or the visual surround were in direct proportion to body-sway angles determined from sway-rod measures at the level of the hip or the shoulder, respectively. Sway-referencing alters the normal relationship between body sway and proprioceptive cues (during support surface sway-referencing) or visual cues (during visual surround sway-referencing) and presumably greatly reduces the contribution of these sensory orientation cues.

For normal subjects, all five stimulus amplitudes were presented for each of the six test conditions, and the stimulus and control trials were presented in a randomized order. Trials with sway-referencing included a 10-s delay prior to stimulus onset during which sway-referencing was active. All eight normal subjects completed a full set of trials with the backboard assembly. Four of these subjects also completed the full set of trials without the backboard assembly (freestanding). Data collection for backboard and freestanding conditions was completed in five testing sessions. Each session lasted about 2 h with one session performed per day. A 5-min break was given between trials.

For VL subjects, testing time was limited. Only backboard trials were performed, and the duration of control trials was reduced (to 130 s) compared with those used for normal subjects. Results from the first VL subject showed that 8° amplitude trials were extremely difficult to complete without falling. Therefore all other VL subjects were presented with 1, 2, and 4° PRTS stimuli. Some VL subjects were unable to complete a 4° trial for a given test condition (Table 2). If this occurred, a 0.5° stimulus was substituted so that results were obtained for each test condition at a minimum of three different stimulus amplitudes. There were three testing sessions for each VL subject lasting about 2.5 h each. Two sessions were performed on the same day (morning and afternoon), and a third session was completed on another day. A 5-min break was given between trials.

All subjects were instructed to maintain a relaxed upright stance position. If a subject fell during a trial, the trial was immediately repeated once or twice. Subjects wore headphones and listened to audio tapes of novels and short stories to mask equipment sounds, maintain alertness, and distract them from concentrating on their balance control.

Transfer function analysis

Results were analyzed primarily by calculating transfer function and coherence function estimates from stimulus-response data from each test trial. A transfer function characterizes the dynamic behavior of a system by showing how response sensitivity (gain) and timing (phase) change as a function of stimulus frequency. At each frequency, the transfer function gain gives the ratio of the amplitude of the response (COM body-sway angle) to the stimulus amplitude (support surface and/or visual surround tilt angle) at that frequency. The transfer function phase (in degrees) expresses the relative timing of the response compared with the stimulus at each frequency.

Transfer functions were computed using a discrete Fourier transform (DFT) to decompose the PRTS stimulus and response waveforms into sinusoidal component parts (Bendat and Piersol 2000). The DFT was applied to each 60.5 s cycle of each trial's stimulus and response waveforms. The DFT was calculated at 150 frequencies ranging from $f = 1/60.5 = 0.0165$ Hz to $f = 150/60.5 = 2.48$ Hz. A property of the PRTS stimulus is that all even frequency components have zero amplitude (Davies 1970). These even frequency points were discarded leaving 75 frequency samples.

Various power spectra were computed and averaged over the N cycles ($N = 6$ or 8)

$$G_x(\omega) = \frac{1}{N} \sum_{i=1}^{N} X_i(j\omega)^* \cdot X_i(j\omega) \tag{2}$$

$$G_y(\omega) = \frac{1}{N} \sum_{i=1}^{N} Y_i(j\omega)^* \cdot Y_i(j\omega) \tag{3}$$

$$G_{xy}(j\omega) = \frac{1}{N} \sum_{i=1}^{N} X_i(j\omega)^* \cdot Y_i(j\omega) \tag{4}$$

where $X_i(j\omega)$ and $Y_i(j\omega)$ are the DFTs of the *i*th stimulus and response cycles, respectively, $\omega = 2\pi f$, j is $\sqrt{-1}$, and * indicates a complex conjugate. Higher-frequency portions of these spectra were further smoothed by averaging adjacent spectral points to produce the final smoothed spectra, $G_{xs}(\omega)$, $G_{ys}(\omega)$, and $G_{xys}(j\omega)$ at 17 frequencies ranging from 0.0165 to 2.23 Hz. (The number of adjacent points averaged increased with increasing frequency such that 15 points contributed to the highest frequency spectral estimate).

The transfer function was then estimated

$$H(j\omega) = \frac{G_{xys}(j\omega)}{G_{xs}(\omega)} \tag{5}$$

and the gain function (ratio of response amplitude to stimulus amplitude) and phase function (in degrees) were computed by

$$|H(\omega)| = \sqrt{H(j\omega)^* \cdot H(j\omega)} \tag{6}$$

$$\angle H(\omega) = \frac{180°}{\pi} \tan^{-1}(\text{Im}(H(j\omega))/\text{Re}(H(j\omega))) \tag{7}$$

where $\mathrm{Im}(H(j\omega))$ and $\mathrm{Re}(H(j\omega))$ are the imaginary and real portions, respectively, of the complex numbers representing transfer function estimates. The phase function was computed using the Matlab (The MathWorks, Natick, MA, version 5.3) function "phase" from the Systems Identification Toolbox. This function "unwraps" the phase values, meaning that phase measures more negative than $-180°$ could be obtained in cases where phase lags were increasing with increasing frequency.

COHERENCE FUNCTION ESTIMATES.   The smoothed power spectra were used to estimate a "coherence function" given by

$$\gamma^2(\omega) = \frac{|G_{xys}(j\omega)|^2}{G_{xs}(\omega) \cdot G_{ys}(\omega)} \tag{8}$$

Values of the coherence function can vary from 0 to 1, with 0 indicating that there is no linear correlation between the stimulus and response, and 1 indicating a perfect linear correlation with no noise. Values less than 1 occur in practice either because there is noise in the system or there is a nonlinear relation between stimulus and response (Bendat and Piersol 2000). Coherence function estimates were also used in the calculation of 95% confidence limits on the transfer function gain and phase data (Otnes and Enochson 1972).

CURVE FITTING.   Transfer function curve fits were made to the experimentally determined transfer function estimates. These curve fits were based on a theoretical model of the postural control system (Fig. 9, *Eqs. 14–17*) and were used to derive estimates of model parameters. The curve fits were made using a constrained nonlinear optimization algorithm ("constr" from the Matlab Optimization Toolbox) that adjusted model transfer function parameters to minimize the error value E given by

$$E = \sum_{i=1}^{P} \frac{|M(j\omega_i) - H(j\omega_i)|}{|M(j\omega_i)|} \tag{9}$$

where $M(j\omega_i)$ and $H(j\omega_i)$ represent the complex value of the model and experimental transfer function, respectively, at the ith frequency point. The error magnitude at each frequency point was summed over the P frequencies included in the fit. The error was normalized by the magnitude of the model to account for the fact that estimation errors were lower for the higher-frequency lower-gain data due to averaging of spectral data. Although 17 frequency points were calculated for experimental transfer functions, P was typically less than 17 (usually 12). The lowest frequency and highest four frequencies were excluded from the fit procedure because the model transfer function was often unable to account for these data. (Large systematic errors between experimental data and fits occurred if all points were included.) Extensive simulations (using the Fig. 9 model and including variability to represent spontaneous body sway) were performed to validate our data analysis and parameter estimation procedures.

RESULTS

Stimulus-evoked body sway

Examples of COM body sway rotational responses to five different amplitudes of the PRTS stimulus for one representative normal subject and one VL subject are shown in Fig. 3. In the example in Fig. 3*B*, the subjects were standing with eyes closed, and the PRTS stimulus was applied to the support surface. The COM sway responses clearly followed the general PRTS stimulus waveform (Fig. 3*A*), indicating that both normal and VL subjects tended to orient to the moving support surface. At the three lowest stimulus amplitudes (0.5, 1, and 2°) for this test condition, the amplitude of body sway was noticeably larger than the stimulus amplitude in both the normal and
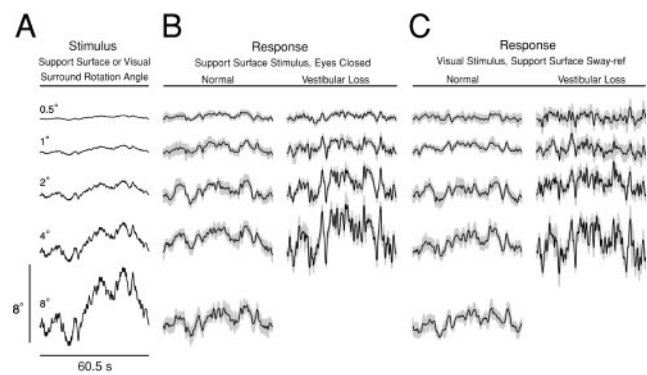

FIG. 3.   Example PRTS stimulus and body-sway responses for normal and vestibular loss subjects. *A*: one cycle of the PRTS stimulus waveform with peak-to-peak amplitude ranging from 0.5 to 8°. *B*: corresponding body-sway responses of a normal and vestibular loss subject to support surface rotations with eyes closed (—, mean of 6 cycles, grayed area represents the 95% confidence interval about the mean). *C*: body-sway responses of a normal and vestibular loss subject to visual surround rotations with the support surface sway-referenced.

VL subjects. In the normal subject, the sway amplitude appeared to saturate as the stimulus amplitude increased, such that the body-sway responses to the two highest stimuli (4 and 8°) were clearly smaller than the stimulus. However, in the VL subject, body sway continued to increase with increasing stimulus amplitude, and body-sway amplitude remained noticeably larger than the stimulus at the highest stimulus amplitude tested (4°). A similar pattern of body-sway responses was seen with the PRTS stimulus applied to the visual surround while subjects stood on a sway-referenced support surface (Fig. 3*C*).

To illustrate the general pattern of responses to all six test conditions, Fig. 4 plots the mean root-mean-square (rms) COM body sway for normal subjects and individual results for the VL subjects. The plots include results for all six test conditions as a function of the peak-to-peak PRTS stimulus amplitude. The rms amplitude of the PRTS stimulus is shown for reference. In the two test conditions where two or more sensory systems were providing veridical orientation cues (i.e., fixed support surface with visual stimulation and fixed visual surround with support surface stimulation), normal subjects showed reduced rms body sway compared with the other test conditions, where fewer sensory systems were providing veridical orientation cues. In the fixed-support-surface condition with visual stimulation, there was no significant difference among mean rms sway for 0.5, 1, 2, and 4° amplitudes for normal subjects, although rms sway was greater for the 8° stimulus compared with the 0.5 or 1° stimuli (Tukey-Kramer multiple comparisons test, $P = 0.05$ significance level). In the fixed-visual-surround condition with support surface stimulation, the mean body-sway response increased in proportion to the stimulus for the 0.5 and 1° amplitudes but then showed no further increase with increasing stimulus amplitude (no significant differences among mean rms sway for 1–8° stimulus amplitudes, Tukey-Kramer multiple comparisons test, $P > 0.05$).

In the four conditions where veridical orientation cues were provided by fewer sensory systems, the mean rms sway amplitude was always greater than the rms stimulus amplitude for 0.5 and 1° stimuli. For stimuli greater than 1°, the rms body-sway response did not increase in proportion to the stimulus. For the 2° stimuli, the mean rms sway amplitude was approx-
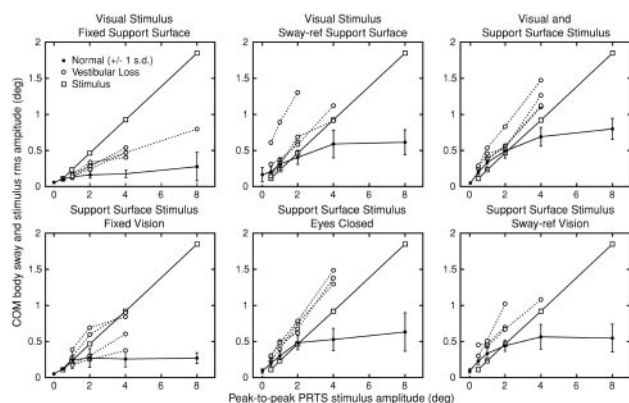
FIG. 4.   Stimulus-response relationships for all 6 test conditions. The root-mean-square (rms) center-of-mass (COM) body sway for normal subjects (●, —, mean ± SD), and rms COM body sway of individual vestibular loss subjects (○, · · ·) are shown as a function of the peak-to-peak stimulus amplitude. The rms amplitude of the PRTS stimulus is shown for reference (□, —).

imately equal to the rms stimulus amplitude. For the 4 and 8° PRTS stimuli, the mean rms sway amplitude was always less than the rms stimulus amplitude. In most conditions, the general pattern of results suggests that the body-sway response saturated, with no further increase in response occurring with PRTS stimuli at or above about 4°. Pairwise multiple comparisons showed no significant difference between 4 and 8° responses in normal subjects ($P > 0.05$, Tukey-Kramer multiple comparisons test).

In contrast, responses of VL subjects generally showed greater levels of stimulus-evoked body sway for each test condition and at each stimulus amplitude, and some subjects were unable to complete all trials (Table 2). Figure 4 plots the rms response amplitudes of individual VL subjects. With the exception of only two individual trials, the individual rms responses of VL subjects were greater than the mean normal responses on all test conditions and at all stimulus amplitudes. In the four test conditions where the number of sensory systems providing veridical orientation cues was reduced, the rms responses of individual VL subjects were always greater than the rms stimulus amplitude, even at the 4° stimulus amplitude where normal subjects showed rms responses that were always less than the stimulus. Overall, the VL subjects' responses increased with increasing stimulus amplitude and showed little evidence for the response saturation seen in normal subjects.

Adaptation and habituation

There was no evidence for adaptation or habituation in normal subjects in their responses to the PRTS stimuli over the six or eight cycles presented in the different test conditions. When cycle by cycle rms sway data from all six test conditions were grouped according to the stimulus amplitude, rather than a decrement in the response due to habituation, the only trends were small increases in the rms response amplitude over the course of the stimulus. Linear regression analyses showed slopes ranging from 0.002°/cycle for the 1° PRTS data to 0.021°/cycle for the 8° PRTS data. The linear regression slope was significantly different from zero only for the 8° PRTS stimulus data ($P < 0.046$). VL subjects also did not appear to habituate to the various stimuli.

Postural control dynamics

Body-sway responses to PRTS stimuli were analyzed using Fourier methods to compute stimulus-response transfer functions (gain and phase as a function of stimulus frequency) and coherence functions. In these transfer functions, a gain measure of one and phase of zero indicates that the body orientation remained perfectly aligned (in amplitude and timing) with the support surface (for tests with support surface stimulus), or with the visual surround (for tests with visual surround stimulus). A gain greater (less) than one at a particular component stimulus frequency indicates that the body sway amplitude was larger (smaller) than the stimulus amplitude at that frequency. A gain of zero indicates that the body orientation was not influenced by the stimulus and remain perfectly aligned with earth-vertical.

EXAMPLE TRANSFER FUNCTIONS.   Figure 5 shows individual transfer functions and their associated coherence functions from four different normal subjects and four different test conditions. All of these transfer functions are from trials where the subjects were restrained to sway as a single-link inverted pendulum by the backboard assembly. The general pattern of gain and phase changes, as a function of stimulus frequency, was similar for all test conditions and stimulus amplitudes. The gain was largest in the 0.1–0.8 Hz frequency range and was often greater than unity in this range. At frequencies less than about 0.1 Hz, the gain gradually decreased with decreasing frequency. At higher frequencies, the gain typically showed a steep decline with increasing frequency. A prominent phase lead was typically present for stimulus frequencies less than about 0.1 Hz. The phase crossed zero in the 0.1–0.2 Hz region and then showed increasing phase lags with increasing frequency. Phase lags of as much as −400° were seen at the highest frequency (2.23 Hz) on some tests (Fig. 5A), but on other tests, the phase lag at the highest frequency was much less (about −200°, Fig. 5B). Coherence functions typically had
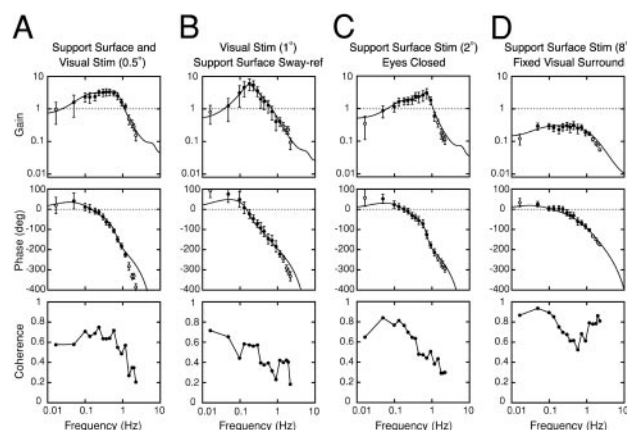

FIG. 5.   Example transfer functions and coherence functions from 4 different stimulus conditions in 4 different normal subjects. Transfer function gain data (log scale) and phase data (linear scale) are plotted against stimulus frequency (log scale). Error bars indicate 95% confidence intervals around the gain and phase estimates (● and ○). Unity gain and 0 phase responses (· · ·) signify the result expected if subjects were able to maintain perfect body alignment to the moving visual surround and/or support surface stimulus. —, fits of *Eq. 14* to the transfer function data. Only transfer function data points indicated by ● were used for the curve fit procedure. Coherence function estimates as a function of stimulus frequency are shown for each test condition. Results are from backboard supported trials.

values in the 0.6–0.8 range at the lower stimulus frequencies, and the values declined with increasing frequency.

The general form of the example transfer functions shown in Fig. 5, *A* and *D,* are representative of the majority of experimentally obtained transfer functions. The two transfer functions in Fig. 5, *B* and *C,* represent the most extreme deviations from the more common transfer function form. Specifically, these two transfer functions show resonant peaks in their gain functions. In one case, a prominent resonant peak was located at about 0.2 Hz. In the other, a smaller resonant peak was located near 0.9 Hz. Of the 240 tests performed by the eight normal subjects, only about 20 tests showed resonant behavior qualitatively similar to the examples shown in Fig. 5, *B* and *C.* Four of the normal subjects did not show resonant behavior on any test. Resonant behavior was most common on test condi-

tions with visual stimulation on a sway-referenced support surface, or with support surface stimulation with eyes closed.

MEAN TRANSFER FUNCTION. *Backboard support.* The mean transfer functions from eight normal subjects are shown in Fig. 6 for the six different test conditions at each of the five different stimulus amplitudes. These transfer function families illustrate that mean gains were greater than unity for all test conditions at the 0.5 and 1° stimulus amplitudes in the 0.1–0.8 Hz frequency range. As the stimulus amplitude increased, the gain generally decreased. For the two visual stimulus conditions with a fixed or sway-referenced support surface, the decrease in gain with increasing stimulus amplitude was more uniform across the bandwidth of test frequencies compared with the other four conditions with support surface stimulation or com-
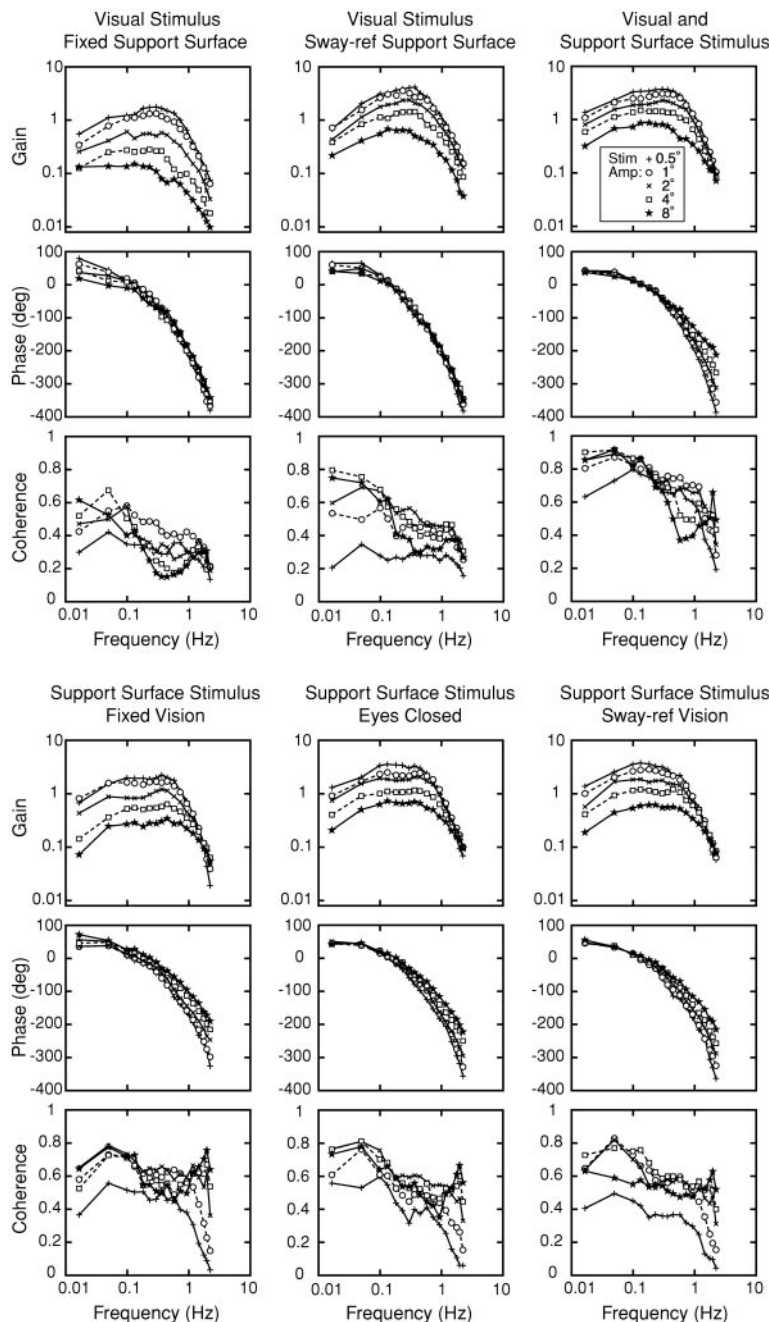

FIG. 6. Mean transfer function gain and phase data, and coherence function data plotted vs. stimulus frequency for the 6 different test conditions and 5 different stimulus amplitudes (mean of data from 8 normal subjects on backboard supported trials).

bined visual and support surface stimulation. In these four support surface stimulus conditions, there was little or no decrease in gain at the highest test frequencies. However, for frequencies less than about 1 Hz, the decline in gain with increasing stimulus amplitude was similar to that for the two visual stimulus conditions. As a result, the gain functions corresponding to the five stimulus amplitudes for all four support surface stimulus conditions converged at about 2 Hz.

Of all test conditions and amplitudes, the largest mean gain value occurred on the 0.5° visual stimulus condition with a sway-referenced support surface. This gain value was 4.1 at a frequency of 0.36 Hz. Among the other tests performed using the 0.5° stimulus amplitude, maximum gains of about 3.7 were obtained on three conditions (support surface stimulation with eyes closed and with sway-referenced vision, and combined support surface and visual stimulation). A lower maximum gain of about 2.2 was obtained with the 0.5° support surface stimulation with fixed vision, and the lowest maximum gain of about 1.8 was obtained with visual stimulation on the fixed support surface.

Phase functions also showed characteristic differences between the two conditions with only visual stimulation and the four conditions with support surface or combined support surface and visual stimulation. For the two conditions with only visual stimulation, the phase functions for all five stimulus amplitudes were indistinguishable from one another for frequencies greater than about 0.1 Hz. Large phase lags ranging from −342 to −382° were measured in these two conditions at 2.23 Hz. For frequencies less than 0.1 Hz, there was some divergence of these phase functions. At the lowest frequency (0.017 Hz) on the fixed support surface with visual stimulus condition, there was a systematic relationship between the phase and stimulus amplitude with the largest phase advance associated with the lowest stimulus amplitude, and the least phase advance occurring with the largest stimulus amplitude.

The phase functions for all conditions with support surface stimulation showed a different pattern. For three of the four support surface stimulus conditions, the phase functions from different stimulus amplitudes were indistinguishable from one another for frequencies less than about 0.1 Hz. (The exception was the fixed vision condition were there was some divergence of phases at lower frequencies, although no systematic relationship between phase and stimulus amplitude was present.) At frequencies greater than about 0.2 Hz, the phase functions associated with different stimulus amplitudes diverged from one another, and this divergence increased with increasing frequency. At a given frequency greater than 0.2 Hz, there was less phase lag associated with larger stimulus amplitudes. The largest difference between mean phases was seen on the combined support surface and visual stimulus condition where the mean phase from the 8° stimulus was −212°, and the mean phase from the 0.5° stimulus was −386° at 2.23 Hz.

Conditions that evoked body sway, using support surface rotation with either eyes closed or sway-referenced visual surround conditions, resulted in very similar responses in normal subjects (Figs. 4 and 6). This suggests that eye closure and visual surround sway-referencing were both equally effective in eliminating the contribution of visual sensory cues to postural control.

Coherence functions were generally largest at the lowest test frequencies and gradually declined with increasing frequency.

Within each of the six test conditions, the coherence function from the 0.5° stimulus typically had lower values than the coherence functions associated with the larger stimulus amplitudes. This is consistent with a lower signal-to-noise ratio for responses evoked by this very low-amplitude stimulus. For 1–8° stimuli, there was no systematic change in coherence with stimulus amplitude for stimulus frequencies less than about 1 Hz. This indicates that each of the responses to the different amplitude stimuli showed a similar degree of linearity even though the overall system responses were clearly nonlinear since gains declined with increasing stimulus amplitude. This suggests that the overall gain decline may be caused by a resetting of system parameters for different amplitudes rather than by a specific nonlinear processing of sensory or motor signals (see DISCUSSION).

One might question the validity of averaging transfer functions across subjects, based on the concern that important individual variations might be obscured or biases introduced. However, examination of each individual's results showed that they were consistent with the population mean. In addition, quantitative estimates of the stiffness and damping properties of each subject's control behavior (see *Model interpretation* section) showed that each subject effectively normalized his or her postural transfer function dynamics by systematically setting stiffness and damping properties in proportion to individual body mass and height parameters. Similar self-normalizing behavior has been reported previously in a study of head stabilization (Keshner et al. 1999).

Freestanding. The major features of transfer and coherence functions obtained with subjects restrained to sway as a single-link inverted pendulum by the backboard support were also observed in freestanding subjects. As an example, the mean transfer and coherence functions from the four subjects who completed a full set of freestanding tests are shown in Fig. 7 for the combined support surface and visual stimulation condition. Both backboard and freestanding gain functions show a decline with increasing stimulus amplitude, and both show the char-
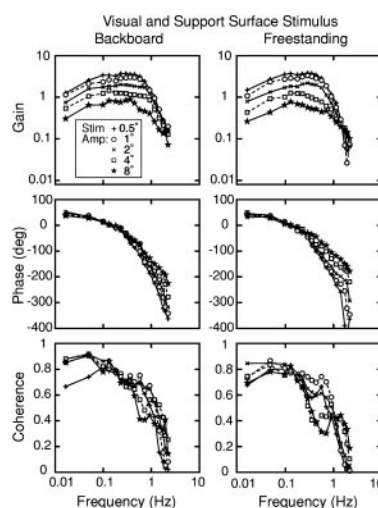

FIG. 7. Comparison of transfer functions and coherence functions obtained in backboard supported (*left*) and freestanding (*right*) conditions. Results are from the combined visual and support surface stimulus condition at 5 different stimulus amplitudes. Each curve represents the mean data from 4 normal subjects who performed both backboard and freestanding trials.

acteristic convergence of the gain functions from different stimulus amplitudes at higher stimulus frequencies.

Both the backboard and freestanding phase functions show a phase lead at frequencies less than 0.1 Hz. The phase functions from different amplitude stimuli were not distinguishable from one another at these lower frequencies. However, as frequency increased greater than about 0.2 Hz, both the backboard and freestanding phase functions diverged from one another, with phase functions showing less phase lag with increasing stimulus amplitude. Coherence functions were also similar for the backboard and freestanding tests.

There was a similar correspondence between backboard-restrained and freestanding results in the other five test conditions. All of the major features of transfer functions for the six test conditions obtained from backboard-restrained subjects (shown in Fig. 6) were also present in the freestanding results.

VL TRANSFER FUNCTIONS. Unlike the normal subject transfer functions, transfer functions derived from VL subjects showed specific characteristic variations between the subjects. These variations precluded any averaging of transfer function results across VL subjects. However, there were some consistent findings across all VL subjects. The most obvious and consistent difference between results from normal and VL subjects was that the transfer function gain functions showed little change with increasing PRTS stimulus amplitude. Figure 8A overlays four transfer functions obtained from one representative VL subject in response to support surface stimulation with eyes closed and PRTS stimulus amplitude varying from 0.5 to 4°. A small decrease in gain can be appreciated by comparing the 0.5° with the 4° data in the lower and mid-frequency range, but this decrease is small compared with the approximate fourfold gain decrease in normal subjects on the same test conditions (see Fig. 6). The phase functions in Fig. 8A also show that there was little change in phase with increasing stimulus amplitude. This is in contrast to the phase data from normal subjects who showed less phase lag with increasing stimulus amplitude in this test condition (Fig. 6).

Results similar to those in Fig. 8A (showing little or no gain reduction or phase changes with increasing stimulus amplitude) were obtained in all four VL subjects with support surface stimulation with eyes closed or sway-referenced vision, with combined support surface and visual stimulation, and with

visual stimulation on a sway-referenced support surface. In contrast to this pattern of results, different VL subjects showed varying amounts of reduction in gain and changes in phase with increasing stimulus amplitude during support surface stimulation with a fixed visual surround. The data from the subject showing the most change are shown in Fig. 8B. For comparison, the data from the VL subjects who showed the least change in this same test condition are shown in Fig. 8C.

The VL subject's transfer function data shown in Fig. 8C also illustrate a property of this subject's responses that distinguished her from the other three VL subjects. Note that all three of the transfer functions from this subject in Fig. 8C are very similar to the transfer function of the other VL subject (Fig. 8B) obtained in response to the 4° PRTS stimulus. That is, the gain functions in Fig. 8C are relatively flat in the low- and mid-frequencies before beginning to decrease at higher frequencies. Additionally, the maximum phase lag in Fig. 8C at the highest frequency is about −280°, which is approximately equal to the phase lag in Fig. 8B at the highest frequency for the 4° stimulus. The pattern of results for the VL subject shown in Fig. 8C (subject VL1) will later be shown to be consistent with this subject maintaining a higher level of postural stiffness than other VL subjects and other normal subjects. This subject's high stiffness strategy was evident in all test conditions.

In the test condition with visual stimulation on a fixed support surface, one of the VL subjects (VL2) showed some reduction in gain with increasing stimulus amplitude, whereas the other three VL subjects did not.

VL subjects generally had more difficulty maintaining balance in the test condition where the visual surround was sway-referenced than in the eyes closed condition. Only one of the four subjects was able to complete the 4° support surface stimulus with a sway-referenced visual surround while three of the four were able to complete the 4° stimulus with eyes closed. Some of the highest gains were obtained on tests with support surface stimulation with sway-referenced vision. An example is shown in Fig. 8D (subject VL2). Subject VL4 was unable to complete any of the tests with the visual surround sway-referenced, including the control test with a fixed support surface, although her performance on all five other test conditions was not distinguishable from the other VL subjects. This poor performance on tests with sway-referenced vision is in
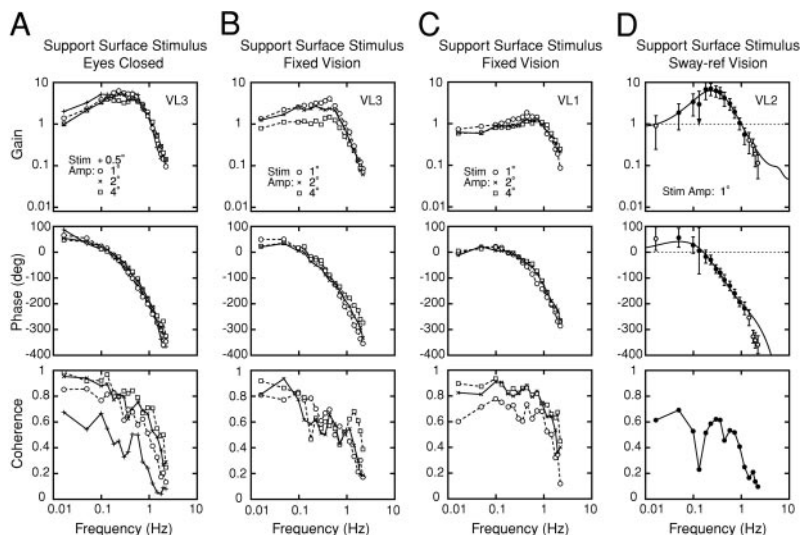

FIG. 8. Example transfer function gain and phase data and coherence function data vs. stimulus frequency from 3 VL subjects. A: results from subject VL3 showing little change in gain and phase functions on tests performed with eyes closed and support surface stimulus amplitudes varying from 0.5 to 4°. B: results from subject VL3 showing a decrease in gain and some change in phase functions when the support surface stimulus amplitude increased from 1 to 4° on tests performed with a fixed visual surround. C: results from subject VL1 performing the same tests as in B but showing little change in gain and phase functions as the stimulus amplitudes varied from 1 to 4°. D: results from subject VL2 showing large mid-frequency gains in response to a 1° support surface stimulus with a sway-referenced visual surround. —, from a fit of Eq. 14 to the transfer function data. Error bars indicate 95% confidence intervals. Only transfer function data points indicated (●) were used for the curve fit procedure. All results are from backboard supported trials.

contrast to the results from normal subjects where performance on tests with eyes closed was indistinguishable from tests with sway-referenced vision (Fig. 6).

Model interpretation

INDEPENDENT CHANNEL MODEL. To achieve further insight into the postural control behavior revealed in the experimental results, we used a simple control system model to parameterize our transfer function results. This "independent channel" model (shown in Fig. 9) uses negative feedback control from sensory systems to generate an active torque, T_a, and muscle/tendon stretch caused by body sway relative to the support surface to generate a passive torque, T_p. T_a and T_p sum to produce the total corrective torque, T_c, acting about the ankle joint. This model assumes that three types of sensory information contribute to the generation of T_a. The sensory information is provided by the visual system, detecting body orientation with respect to the visual environment, proprioceptive system, detecting body orientation with respect to the support surface, and graviceptive system, detecting body orientation with respect to earth vertical. All sensory channels act separately, and the "goal" of each channel is to minimize deviation from its individual internal reference.

The body rotation produced by T_c is described by the differential equation of a single-link inverted pendulum

$$J \frac{d^2 \text{BS}}{dt^2} = mgh \sin(\text{BS}) + T_c \qquad (10)$$

where J is the body's moment of inertia about the ankle joint axis, m is body mass (not including the feet), g is acceleration due to gravity, h is the height of the COM above the ankle joint, and BS is the angular position of the body with respect to earth vertical. Both BS and T_c are time varying. Expressing this equation as a Laplace transform gives

$$\frac{\text{BS}(s)}{T_c(s)} = \frac{1}{Js^2 - mgh} \qquad (11)$$

where s is the Laplace variable and the small angle approximation $\text{BS} \approx \sin(\text{BS})$ was used to simplify the equation.

An inverted pendulum is inherently unstable because a small deviation of body position from a perfect upright position produces a torque due to gravity, $mgh \sin(\text{BS})$, that accelerates the body further from upright. To counteract this gravitational torque, T_c must be generated with a sign opposite to the gravitational torque. The stability and dynamic behavior of the

inverted pendulum control depends on the time course of T_c. If we assume initially that the passive torque contribution to T_c is negligible, then all of the stabilizing torque must be derived from the sensory error signal, e, given by

$$e(t) = -w_g \text{BS}(t) - w_v[\text{BS}(t) - \text{VS}(t)] - w_p[\text{BS}(t) - \text{FS}(t)] \qquad (12)$$

It is known from control system theory that stabilization of an inverted pendulum requires that T_a minimally contain two components: one proportional to e (a "stiffness" factor) and a second proportional to the time derivative of e (a "damping" factor). An optional third component contributes a torque proportional to the mathematical time integral of e. This integral component adds low frequency error correcting properties to the overall control system but is not necessary for stability. The equation for a controller that contains all three of these components is

$$T_a(t) = K_P e + K_D \frac{de}{dt} + K_I \int e \, dt \qquad (13)$$

where t is time, and K_P, K_D, and K_I are gain constants that determine the magnitude of the position, velocity, and integral components, respectively. This type of controller, commonly used in man-made control systems, is referred to as a PID controller (proportional, integral, derivative control).

If all of the sensory systems are assumed to have no dynamic behavior over the bandwidth of movement associated with body sway, then the overall transfer function relating body sway evoked by either visual surround and/or support surface motion is given by

$$\frac{\text{BS}(s)}{\text{VS}(s)} \quad \text{or} \quad \frac{\text{BS}(s)}{\text{FS}(s)} = \frac{W(K_D s^2 + K_P s + K_I)e^{-\tau_d s}}{Js^3 - mghs + (K_D s^2 + K_P s + K_I)e^{-\tau_d s}} \qquad (14)$$

where VS is the rotational position of the visual surround in space, FS is the foot-in-space rotational position (equal to the support surface rotational angle), and τ_d is a time delay that includes sensory transduction, neural processing, transmission, and muscle activation delays.

Passive torque may not be negligible. T_p could contribute to T_c in test conditions where there is body movement relative to the feet (i.e., where BF, defined in Fig. 9, varies over time). This passive torque is assumed to contain both a stiffness component, K, and a damping component, B, and it acts without a time delay. The overall transfer function for conditions with support surface stimulation or combined visual and support surface stimulation is given by
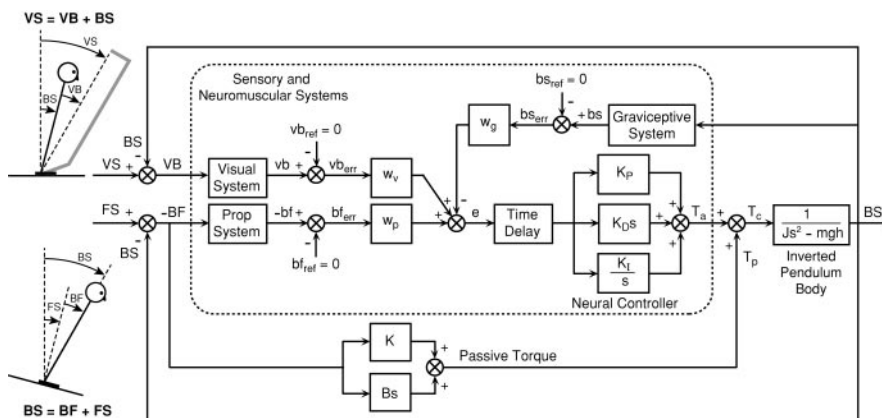

FIG. 9. "Independent channel" model of sensory integration in postural control showing a weighted addition of contributions from visual, proprioceptive, and graviceptive systems to the generation of an active corrective torque, T_a, as well as a passive torque contribution, T_p, related to body movement relative to the feet.

$$\frac{\text{BS}(s)}{\text{FS}(s)} = \frac{Bs^2 + Ks + W(K_D s^2 + K_P s + K_I)e^{-\tau_d s}}{Js^3 + Bs^2 + (K - mgh)s + (K_D s^2 + K_P s + K_I)e^{-\tau_d s}} \quad (15)$$

and for the condition with visual stimulation on a fixed support surface

$$\frac{\text{BS}(s)}{\text{VS}(s)} = \frac{W(K_D s^2 + K_P s + K_I)e^{-\tau_d s}}{Js^3 + Bs^2 + (K - mgh)s + (K_D s^2 + K_P s + K_I)e^{-\tau_d s}} \quad (16)$$

In *Eqs. 14–16,* the parameter W is a factor that influences the overall gain of the transfer function but does not influence the phase. We refer to W as the "sensory weighting factor" because W is a function of the sensory channel weights in the different test conditions. Specifically, in the condition with support surface stimulation with eyes closed or sway-referenced vision, $W = w_p = 1 - w_g$, where w_p and w_g are the proprioceptive and graviceptive channel weights, respectively. (We assume that the sum of all sensory channels that are contributing to balance control is unity in steady state conditions, in this case $w_p + w_g = 1$.) For the test condition with visual stimulation on a sway-referenced support surface, $W = w_v = 1 - w_g$. For visual stimulation on a fixed support surface, $W = w_v = 1 - w_p - w_g$. For support surface stimulation with fixed visual surround, $W = w_p = 1 - w_v - w_g$. Finally, for combined support surface and visual stimulation, $W = w_v + w_p = 1 - w_g$. Therefore, estimates of W obtained from transfer function data can be used to derive estimates of the relative contributions made by different sensory systems to balance control in different test conditions with different stimulus amplitudes.

Although the Fig. 9 model represents the output of the sensory systems as position signals, this is not meant to imply that the postural control system makes use of only position information. This model could be equivalently drawn to include both position and velocity signals (as well as other functions of body motion) derived from the sensory systems, and the active corrective torque would then be generated by appropriately scaling and summing the individual motion signals.

Despite the various simplifying assumptions, the independent channel model can explain experimental transfer function results over a wide range of test frequencies, as illustrated by the curve fits of *Eq. 14* to transfer function data shown in Figs. 5 and 8D. These curve fits show that the experimental gain and phase data over a frequency range of about 0.05–1.2 Hz are consistent with *Eq. 14,* including results from some tests that showed prominent resonant properties. Limitations of this model were evident in that gain and phase results below and above this frequency range were not always well fit by *Eq. 14.* These limitations were not overcome by inclusion of passive properties (*Eqs. 15* or *16*).

Curve fits were made to all individual transfer function curves of normal and VL subjects and to the average transfer function data from normal subjects using *Eq. 14* (no passive torque) and *Eqs. 15* or *16* (including passive torque). To limit the number of unconstrained fit parameters, we used anthropometric estimates of J and h (Winter 1990) and direct measurement of m (less 2.6% of total m to account for mass of the feet). For curve fits to transfer function data obtained using the backboard restraint, the values of J, h, and m included the backboard contribution.

Curve fits using *Eq. 14* reliably converged to single solutions. Results from these curve fits are discussed in the following text. Later we describe estimates of passive stiffness, K, and damping parameters, B, derived from curve fits of *Eqs. 15* and *16.*

PARAMETER VARIATION WITH STIMULUS AMPLITUDE. The mean transfer function data shown in Fig. 6, from the eight normal subjects, were fit with *Eq. 14* using the means of the parameters J, m, and h for these subjects ($J = 81.1$ kg m², $m = 83.3$ kg, $h = 0.896$ m; all of these parameters included the backboard contribution). Figure 10 (*left*) shows the variation in W, K_P, K_D, and τ_d as a function of the PRTS stimulus amplitude for the six test conditions. These results, for mean normal transfer function data, are consistent with the results of fits to the transfer function data from each of the individual normal subjects (not

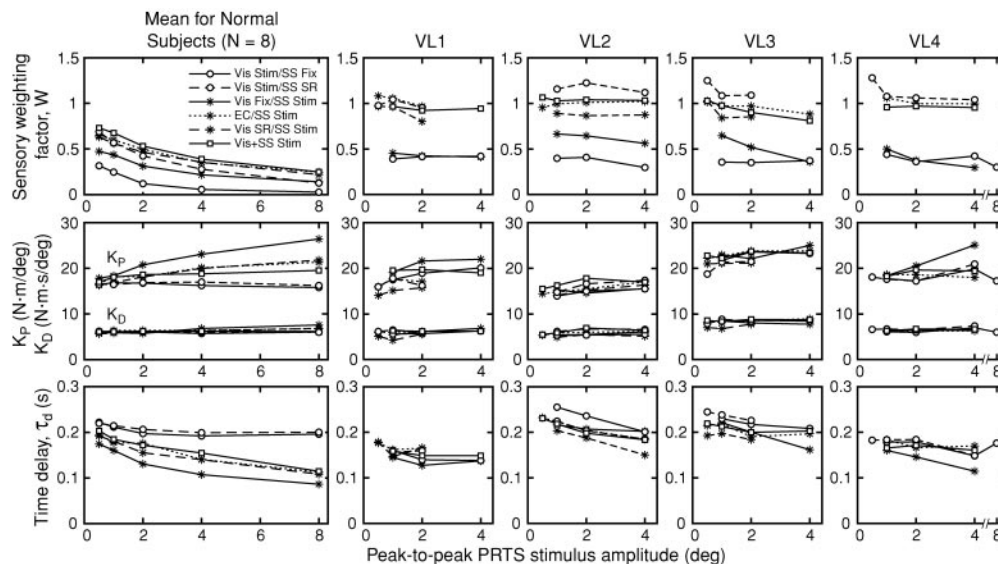FIG. 10. Independent channel model parameters as a function of stimulus amplitude for the 6 test conditions shown in Table 2. Parameter estimates for normal subjects (*left*) were obtained from curve fits of *Eq. 14* to the mean transfer function data shown in Fig. 6. Parameter estimates for the 4 VL subjects (*columns VL1–VL4*) were obtained from curve fits of *Eq. 14* to their individual transfer function data.

shown). The mean K_I was 2.2 ± 1.2 (SD) Nm s^{-1}deg^{-1} for all fits to the mean transfer functions for all conditions and stimulus amplitudes. There was considerable variation in K_I among the different subjects (see also Fig. 12). The K_I results are not plotted since the trends in K_I values from the fits to the mean normal transfer function were not necessarily representative of results from individual subjects.

Also shown in Fig. 10 are results from the four VL subjects. These results were obtained from fits to the transfer function data from individual trials of the six test conditions. The results were not averaged because there was a wider variation of results among the VL subjects compared with normal subjects. Some data points are missing because VL subjects were unable to complete some tests with 4° PRTS stimuli, and *subject VL4* was unable to complete any of the trials where the visual surround was sway-referenced.

For normal subjects, the sensory weighting factor, W, declined with increasing stimulus amplitude for all test conditions. The decline in W is indicative of the general decrease in transfer function gain with increasing stimulus amplitude seen in Fig. 6. In contrast to normal subjects, VL subjects showed little and, sometimes, no decrease in W with increasing stimulus amplitude in most test conditions. There were some exceptions. In particular, *subject VL3* showed a large decline in W with stimulus amplitude for tests with support surface stimulation with a fixed visual surround (transfer function data shown in Fig. 8*B*), and smaller declines in other conditions (support surface stimulation with eyes closed and combined support surface and visual surround stimulation). The other three VL subjects also showed small declines in W with stimulus amplitude on various individual test conditions.

For normal subjects, the largest value of $W = 0.73$ was obtained with the lowest amplitude PRTS stimulus in the condition with both support surface and visual stimulation. Slightly smaller values of W were obtained in the three other conditions where orientation cues were limited by eye closure or by sway-referencing of the visual surround or support surface. At any given stimulus amplitude, the smallest value of W was always obtained for visual stimulation on a fixed support surface.

For VL subjects, the value of W was close to unity for the four conditions where sensory orientation cues were limited by eye closure or by sway-referencing of the visual surround or support surface, and in the condition with combined support surface and visual surround rotation. In these four test conditions, the mean value of W over all stimulus amplitudes was 1.00 ± 0.10 (SD). The value of W obtained with visual surround rotation on a fixed support surface varied little with stimulus amplitude and, in most cases, was larger than the largest W value obtained from the mean normal results in the same test condition. In two of the four VL subjects (*VL1* and *VL4*), the values of W were nearly identical in the conditions with visual stimulation with fixed support surface, and support surface stimulation with fixed vision. This pattern of results differs from normal subjects who always showed lower values of W in the visual stimulus condition with fixed support. The other two VL subjects (*VL2* and *VL3*) showed a pattern that more closely resembled the pattern seen in normal subjects.

For normal subjects, the active stiffness parameter, K_P, increased with the stimulus amplitude in some conditions but not in others. Specifically, K_P did not vary with stimulus amplitude

in conditions where the stimulus was provided only by visual surround rotation. (Repeated-measures ANOVA of K_P values from curve fits to transfer functions of all eight normal subjects showed no significant difference among mean K_P for 0.5–8° visual surround stimuli, $P > 0.2$.) In all conditions where the stimulus was provided by support surface rotation, or by combined support surface and visual surround rotation, K_P increased with increasing stimulus amplitude (the hypothesis of equal K_P means rejected by repeated-measures ANOVA, $P < 0.002$). This increase was largest for support surface stimulation while viewing a fixed visual surround. In this condition with the 8° PRTS stimulus, K_P was 1.65 times the value of K_P in the visual stimulus conditions. Less of an increase with stimulus amplitude occurred with eye closure or sway-referenced vision and still less with combined support surface and visual surround stimulation. The values of K_P obtained at low stimulus amplitudes (0.5 or 1°) were nearly the same for all six test conditions.

The results of K_P variations with stimulus amplitude and test condition were more variable among the four VL subjects. In contrast to the results from normal subjects, two of the four VL subjects (*VL1* and *VL3*) showed some increase in K_P with stimulus amplitude for conditions where the stimulus was provided only by visual surround rotation. Also in contrast to normal subjects, there was generally no clear difference among test conditions in the variation of K_P with stimulus amplitude, although the largest values of K_P usually occurred at the highest stimulus amplitude tested. *Subjects VL1* and *VL4* did show results similar to normal subjects in that the largest K_P values were obtained at the largest stimulus amplitude in the condition with support surface rotation with fixed vision.

Similar to K_P, the damping parameter, K_D, in normal subjects showed essentially no variation with stimulus amplitude in the two test conditions with visual surround stimulation (fixed and sway-referenced surface). Additionally, K_D did not change with amplitude on the combined visual and support surface stimulus condition. (Repeated-measures ANOVA of individual K_D values showed no significant difference in means for 0.5–8° visual surround or combined visual and support surface stimuli, $P > 0.5$.) Although not evident in Fig. 10, K_D did increase in normal subjects in the three conditions with only support surface stimulation (repeated-measures ANOVA of individual K_D values, $P < 0.006$), although this increase was proportionally smaller than the K_P increase in the same test conditions. The largest K_D increase was in the fixed vision condition where the mean K_D was 1.33 times larger in the 8° compared with the 0.5° support surface test. The individual transfer functions from all four of the VL subjects showed only small variations in K_D with changing stimulus amplitudes and conditions (Fig. 10) even though K_P often increased with increasing amplitude. The proportionally greater change in K_P compared with K_D with stimulus amplitude that occurred in many test conditions for both normal and VL subjects was unexpected. In a closed-loop control system, an increase in K_P without a corresponding increase in K_D would be expected to produce resonant behavior. However, resonant behavior was not typically observed.

A second unexpected finding showed why resonant behavior did not typically occur. The apparent time delay, τ_d, of the control loop changed as a function of stimulus amplitude and was also dependent on the stimulus condition. This change in

τ_d changed the effective control loop damping and apparently compensated for changes in K_P (see DISCUSSION). For normal subjects in the two conditions where only visual surround rotation was providing the stimulus, the mean τ_d was 206 ± 11 (SD) ms across all amplitudes of these two conditions, and there was only a small decrease in τ_d with increasing amplitude. For the other four test conditions, τ_d was smaller than for the visual stimulus conditions at all stimulus amplitudes, and there was a large decrease in τ_d with increasing stimulus amplitude. For these four conditions, the mean τ_d was 191 ms at the 0.5° stimulus amplitude and decreased to 105 ms at the 8° amplitude. Of these four conditions, τ_d was smallest for the condition with support surface stimulation and a fixed visual surround. Recall that this is the same condition that showed the largest K_P measures. Although the extent of τ_d change with amplitude varied with the test condition, repeated-measures ANOVA performed on individual τ_d measures rejected the hypothesis of equal τ_d means across stimulus amplitudes, even in the two conditions with only visual stimulation (repeated-measures ANOVA, $P < 0.005$).

Among the four VL subjects, τ_d changes with stimulus amplitude and test condition were more variable compared with the normal subjects. Two of the VL subjects (*VL1* and *VL4*) showed little change in τ_d with stimulus amplitude in most test conditions (except for support surface rotation with fixed vision for *subject VL4*). *Subjects VL2* and *VL3* showed a trend toward decreasing τ_d with increasing stimulus amplitude. This trend was present for both visual stimulus conditions and support surface stimulus conditions.

ESTIMATES OF PASSIVE STIFFNESS AND DAMPING. In most cases, fits to the mean transfer function data using *Eqs. 15* and *16* produced results with slightly reduced error (E in *Eq. 9*) compared with the *Eq. 14* fits. However, some of the *Eq. 15* and *16* fits resulted in larger errors or converged to parameters that were quite different from parameters obtained on closely related trials. When these apparently unreliable fits were excluded, there remained a total of 14 fits of *Eq. 15* to the 20 trials with support surface stimulation only or combined visual and support surface stimulation and 4 fits of *Eq. 16* to the 5 trials with visual stimulation on a fixed support surface.

For the *Eq. 15* fits, the mean passive stiffness parameter, K, was 1.6 ± 0.5 Nm deg^{-1} (range 0.7–2.3). There was some tendency for K to increase with increasing stimulus amplitude. The mean active stiffness parameter, K_P (16.9 Nm deg^{-1}), identified from the *Eq. 15* fits, was about 10 times larger than K. The corresponding mean K_P value from *Eq. 14* fits (18.6 Nm deg^{-1}) was very close to the sum of K and K_P from the *Eq. 15* model. For the *Eq. 16* fits, the mean value of passive stiffness parameter, K, was 2.1 ± 0.4 Nm deg^{-1} (range 1.5–2.6).

For the *Eq. 15* fits, the mean passive damping parameter, B, was 0.43 ± 0.19 Nm s deg^{-1} (range 0.16–0.75). There was no clear change in B with increasing stimulus amplitude. The mean active damping parameter, K_D (5.8 Nm s deg^{-1}), identified from the *Eq. 15* fits, was about 13 times larger than B. The corresponding mean K_D value (6.1 Nm s deg^{-1}) from *Eq. 14* fits was close to the sum of B and K_D from the *Eq. 15* model. For the *Eq. 16* fits, the mean value of passive damping parameter, B, was 3.3 ± 0.7 Nm s deg^{-1} (range 2.5–4.3). The mean active damping parameter, K_D (5.0 Nm s deg^{-1}), identified from the *Eq. 16* fits, was only 1.5 times larger than B on these

trials, suggesting that passive damping may contribute more to overall damping when the surface is fixed than when it is moving.

TIME DELAY VARIATION WITH STIFFNESS. The results from normal subjects in Fig. 10 suggest that τ_d may be related to K_P because tests producing smaller values of τ_d typically gave larger values of K_P. This correlation is evident in plots of τ_d versus K_P shown in Fig. 11. Figure 11*A* shows K_P and τ_d parameters obtained from curve fits to transfer functions of 30 different tests (6 conditions times 5 stimulus amplitudes) for three representative normal subjects. The data from all eight normal subjects suggest that a linear relation exists between τ_d and K_P.

Linear regressions were performed on the τ_d versus K_P data from curve fits to the mean normal transfer functions and from curve fits to the individual transfer functions. The regression slope of the τ_d versus K_P data from fits to the mean normal transfer functions was −14.4 ms/Nm deg^{-1}. For the individual normal subjects, the regression slopes ranged from −10.1 to −18.4 ms/Nm deg^{-1} and had a mean of −13.8 ± 3.6 ms/Nm deg^{-1}. The τ_d versus K_P correlation coefficient, r, for data derived from the mean transfer functions was $r = -0.92$. For the individual τ_d versus K_P data, r ranged from −0.76 to −0.92 and had a mean of −0.84.

VL subjects also showed some correlation between τ_d and K_P. Data from three of the VL subjects are shown in Fig. 11*B* (the fourth subject's data partially overlapped with *subject VL1*'s data, and was not included for clarity). In general, the correlation coefficients for the VL results were lower than results from normal subjects (mean $r = -0.73$, range −0.54 to −0.92). These generally lower correlations appear to be due to
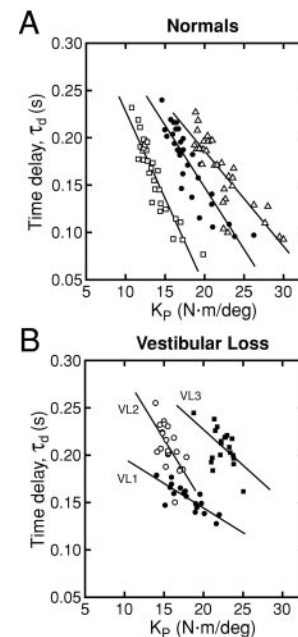
FIG. 11. Variation in the independent channel model time delay parameter, τ_d, with stiffness, K_P, and as a function of stimulus amplitude. *A*: relationship between τ_d and K_P for three representative normal subjects. Parameters were obtained from curve fits to transfer functions from all 30 tests performed by backboard supported normal subjects. —, linear regression fits with associated correlation coefficients of $r = -0.92$ (□), −0.89 (●), and −0.84 (△). *B*: relationship between τ_d and K_P for 3 of the 4 vestibular loss subjects. Correlation coefficients were $r = -0.81$ (*VL1*), −0.63 (*VL2*), and −0.54 (*VL3*).

the fact that two of the four VL subjects (*VL2* and *VL3*) showed relatively little variation in K_P across the various test conditions. The correlation values for the other two VL subjects, whose K_P measures did vary more across test conditions, were compatible with the results from normal subjects.

The linear regression slopes of the τ_d versus K_P data for three of the four VL subjects were smaller in magnitude than any of the regression slopes for normal subjects. The regression slopes for these three subjects ranges from -5.2 to -8.9 ms/Nm deg^{-1}. The fourth VL subject (*VL2*) had a regression slope close to the mean of normal subjects.

PARAMETER VARIATION WITH SUBJECT MASS. Stiffness, K_P, and damping, K_D, were strongly correlated with subject mass, moment of inertia, and other related body mass measures. In contrast, the integral control factor, K_I, showed only a weak correlation, and time delay, τ_d, was essentially uncorrelated with measures of mass and moment of inertia. Figure 12 plots these various parameters versus the product of subject mass and COM height. The mass times COM height product is related to the amount of destabilizing torque due to gravity associated with deviation of body orientation from a perfect upright position.

The data in Fig. 12 include results from the eight normal subjects who performed tests with the backboard restraint, the four VL subjects with backboard restraint, and the subset of the four normal subjects who also performed tests in a freestanding condition. For the tests performed with the backboard, the measures included the added mass of the backboard, and the COM height measure included the effect of the backboard on overall COM height, which slightly lowered the COM height compared with the freestanding subject. Each data point in Fig. 12 represents the mean value of the control parameters obtained from curve fits to transfer function data of the six different test conditions using 1° PRTS stimuli. Results from

the 1° PRTS stimuli were used because, at this low stimulus amplitude, there tended to be a convergence of K_P and τ_d measures to a common value independent of the test condition (see Fig. 10), and a full set of results from VL subjects was available at this stimulus amplitude. Figure 12 plots (——) the results of linear regression analysis performed on the mean data values from the eight backboard-restrained normal subjects. The correlation coefficients shown apply to these same data.

The K_P measures show a high correlation with mass times COM height ($r = 0.97$ for data from backboard-restrained normal subjects). The minimal torque required to overcome the destabilizing torque due to gravity is represented as - - -. The difference between each subject's K_P value and the dashed line represents the amount of corrective torque that is in excess of the minimal amount required to maintain stance. In some sense, this represents a "safety factor" of actively generated corrective torque. The regression line K_P intercept was close to zero, and its slope [0.226 (Nm deg^{-1})/(kg m)] was slightly greater than the minimal torque line [0.171 (Nm deg^{-1})/(kg m)]. This indicates that larger mass subjects maintained a proportionally larger safety factor than lower mass subjects [i.e., K_P/(minimum K_P) ≈ 1.3 independent of subject mass].

The K_P data from the four freestanding normal subjects remained very close to the regression line for the K_P data from the eight backboard-restrained subjects. This indicates that these four subjects altered their K_P to account for the change in mass/moment of inertia associated with use of the backboard.

The K_P data from the VL subjects were also reasonably close to the regression line for the K_P data from normal subjects. However, one of the four VL subjects (*VL1*) had a mean K_P value that was noticeably larger than normal subjects with similar body mass. A second VL subject (*VL4*) also had a somewhat larger mean K_P. These differences compared with normal subjects will be more evident when normalized values of K_P are considered later.

The K_D data from normal subjects (freestanding and with backboard) and VL subjects also were highly correlated with body mass times COM height. The linear regression line and correlation coefficient ($K_D = 0.0871\ mh - 0.463$, $r = 0.95$) shown for the K_D data in Fig. 12 (*top right*) are for the mean K_D data from backboard-restrained normal subjects on 1° PRTS tests. The mean K_D results from the four freestanding normal subjects were close to the linear regression line, again indicating that subjects adjusted their K_D to account for altered body dynamics due to backboard use. The mean K_D values from VL subjects were also close to the regression line for normal subjects.

The time delay measure, τ_d, showed essentially no variation with body mass measures (Fig. 12, *bottom right*). There was no change in τ_d noted in the normal subjects who performed tests both with and without the backboard. However, the mean τ_d measures from the VL subjects deviated from the normal subject τ_d results. The two subjects with the largest mean τ_d measures were both VL subjects (*VL2* and *VL3*). The two subjects with the smallest mean τ_d measures were also both VL subjects (*VL1* and *VL4*). Note that the two subjects with the smallest τ_ds also had relatively large K_P measures. This combination of results suggests that these subjects were maintaining an overall increased level of stiffness, possibly as a strategy for compensating for their vestibular deficit. However, in-
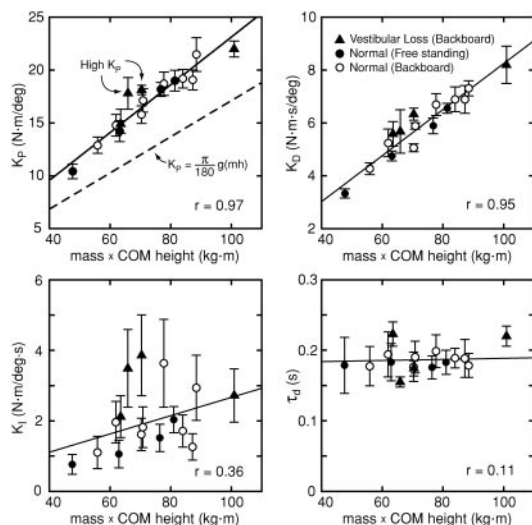
FIG. 12. Neural controller parameters (K_P, K_D, K_I) and time delay (τ_d) as a function of body mass times COM height for normal subjects with backboard support (○) and free-standing (●), and for vestibular loss subjects with backboard support (▲). Parameter estimates (means ± SD) were derived from curve fits of *Eq. 14* to transfer function data from 1° PRTS stimuli for the 6 test conditions in Table 2. ——, linear regression fits to mean data from backboard supported trials in normal subjects. Correlation coefficients are also calculated from the mean data from backboard supported trials in normal subjects. - - -, the minimum level of stiffness compatible with stability.

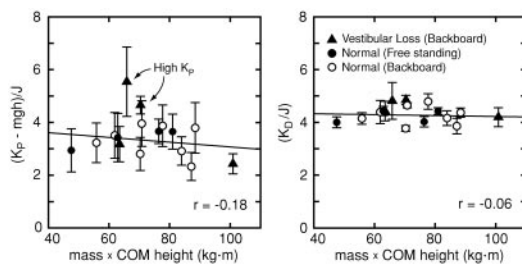FIG. 13. Normalized stiffness (*left*) and damping factors (*right*) as a function of subject mass times COM height for normal subjects both freestanding (●) and backboard supported (○) and vestibular loss subjects with backboard support (▲). Mean (± SD) results are from the 6 different test conditions at 1° PRTS stimulus amplitude. K_P and K_D are expressed in radian units for these normalized calculations. The correlation coefficients and linear regression lines are calculated from the mean data of 8 backboard supported normal subjects.

creased stiffness requires increased damping to avoid resonant behavior. This increased damping was provided not only by slightly increased values of K_D for these subjects but also by a decrease in apparent time delay.

Finally, K_I measures showed large variability, and only a weak correlation with body mass measures (Fig. 12, *bottom left*). This parameter accounts for the low-frequency phase advance and gain decline seen in the experimental transfer functions. The transfer function given by *Eq. 14* often did not fit the low-frequency data well. The large variability in K_I may reflect the fact that this parameter does not provide a complete explanation for the observed low-frequency behavior.

NORMALIZED STIFFNESS AND DAMPING COEFFICIENTS. If *Eq. 14* is simplified by ignoring the effects of K_I and time delay (set K_I and τ_d to 0) and dividing the numerator and denominator by the subject's moment of inertia, J, then the denominator is given by $s^2 + (K_D/J)s + (K_P - mgh)/J$. Setting the denominator equal to zero gives the characteristic differential equation relating the body-sway response, BS, to the stimulus, either VS or FS. The characteristic equation is an important determiner of the dynamic properties of the system. Therefore if the normalized stiffness and damping factors of this equation, $(K_P - mgh)/J$ and K_D/J, respectively, are similar across subjects, then this implies that the transfer function dynamic properties are also similar across subjects.

Figure 13 plots these normalized stiffness and damping factors for the eight normal subjects (with backboard, ○), the four VL subjects (with backboard, ▲), and the subset of four normal subjects who performed the tests freestanding (●). All data are from tests with 1° PRTS amplitudes, and each point is the mean of results from the six different test conditions. The regression lines and correlation coefficients are determined from the mean data from the eight normal subjects who performed tests with the backboard. The results show that there is little variation among normal subjects in the normalized stiffness and damping factors. The normalized stiffness and damping factors determined in the freestanding condition were not distinguishable from those determined with the backboard. The limited variation in these normalized parameters indicates that the general dynamic behavior varied little among the normal subjects despite the wide range of body mass, height, and moment of inertia. Therefore little or no distortion resulted from the averaging of transfer function data across subjects (Figs. 6 and 7), and the transfer function parameters derived

from curve fits to the mean transfer functions accurately reflect the mean behavior of the population.

The normalized stiffness and damping factors for VL subjects did show some differences compared with normal subjects. The largest two normalized stiffness factors were both from VL subjects (*VL1* and *VL4*). The mean normalized damping factors for these two subjects were also greater than for any normal subject or the other two VL subjects, although these values were only slightly greater than the largest values from normal subjects.

VARYING CONTRIBUTIONS OF SENSORY CHANNELS. In the previous description of the independent channel model, it was stated that the sensory channel weighting factor, W, could be used to derive estimates of the relative contributions (w_v, w_p, and w_g) made by different sensory systems to balance control in different test conditions and with different stimulus amplitudes. The derivation of these estimates assumes that, in steady-state conditions, the sum of the weights from all sensory channels that are contributing to postural control is unity. The derivation also assumes that sway-referencing of the visual surround or support surface effectively eliminates the contribution of visual or proprioceptive sensory cues, respectively (i.e., VB = 0 or BF = 0 in the Fig. 9 model).

The graphs in Fig. 14 show the change in sensory channel weights as a function of PRTS stimulus amplitude as derived from different test conditions using the backboard support. The mean results from normal subjects are represented by ○ and ●. Results from individual example VL subjects are also shown (× for *VL3* and △ and ▲ for *VL2*). The *left column* shows w_v, the *middle column* w_p, and the *right column* w_g.

The results in the top row were derived from W values for tests where the stimulus was provided by visual surround motion while the subject stood on a sway-referenced support surface. In this case, $w_v = W$, $w_g = 1 - w_v$. In this condition, the visual contribution to postural control for normal subjects was largest ($w_v = 0.77$) at the lowest stimulus amplitude. The contribution of the visual channel steadily decreased with increasing stimulus amplitude such that at the highest stimulus amplitude, postural control was dominated by the contribution from graviceptors ($w_g = 0.87$, $w_v = 0.13$).

For the example data from the VL subject (*VL2*) shown in Fig. 14, *top*, we also assumed that $w_v = W$ and $w_g = 1 - w_v$. If the graviceptor contribution was entirely provided by vestibular-derived sensory cues, then we would expect to find that $w_v = 1$ and $w_g = 0$, independent of stimulus amplitude. This was approximately the case for this subject except that w_v was actually slightly greater than 1 (mean $w_v = 1.17$). This gave a seemingly nonsensical mean w_g of -0.17. It is uncertain if there is any physiological significance to these unexpected values, but similar results were obtained for three of the four VL subjects in this test condition (as can be surmised from W values shown in Fig. 10 for the individual VL subjects). One could speculate that the assumption of $w_v + w_g = 1$ is not valid, and this subject was able to derive some orientation information from support surface cues (possibly due to imperfections in sway-referencing of the support surface or due to nonvestibular graviceptors).

Figure 14, *middle row,* shows the results for normal subjects from tests with a support surface stimulus and either eyes closed (● and —) or sway-referenced vision (○ and - - -). The
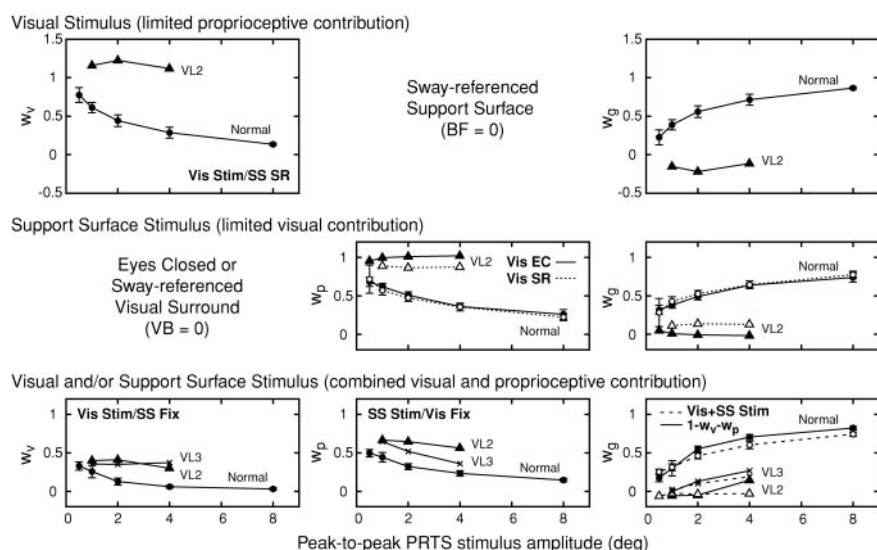
FIG. 14. Changes in sensory channel weights as a function of stimulus amplitude in different test conditions. Weights were derived from curve fits of *Eq. 14* to transfer function data with the assumption that the weights of all sensory channels contributing to postural control in a given condition sum to unity. Results for normal subjects show mean values ($\pm$ SD) ($\bullet$ and $\circ$). Individual results are shown for 2 VL subjects ($\blacktriangle$ and $\triangle$ for *VL2* and $\times$ for *VL3*). *Left*: visual channel weight, w_v. *Middle*: proprioceptive channel weight, w_p. *Right*: graviceptive channel weight, w_g. *Top*: results when only visual and graviceptive cues contribute to postural control (visual stimulus on sway-referenced support surface). *Middle row*: results when only proprioceptive and graviceptive cues contribute to postural control [support surface stimulus with eyes closed (—) or with sway-referenced vision ($\cdots$)]. *Bottom*: results when visual, proprioceptive, and graviceptive channels contribute to postural control [w_v derived from visual stimulus trials performed on fixed support surface, w_p derived from support surface stimulus performed with fixed visual surround, and w_g derived either from combined support surface and visual surround stimulus (- - -) or from the relation $w_g = 1 - w_v - w_p$ (—)].

results for these two test conditions for normal subjects were nearly identical. In this condition, $w_p = W$, $w_g = 1 - w_p$. At the lowest stimulus amplitude, proprioceptive cues provided the major contribution to postural control ($w_p = 0.70$, $w_g = 0.30$) while at the highest stimulus amplitude, the contribution of graviceptive cues dominated ($w_p = 0.24$, $w_g = 0.76$). These results were similar to the visual stimulation results described previously. However, with support surface stimulation, there was a smaller shift from proprioceptive to graviceptive contributions than occurred with visual stimulation.

The results for the example VL subject were somewhat different for tests with eye closure compared with sway-referenced vision (Fig. 14, *middle row*, $\blacktriangle$ and — for eyes closed, $\triangle$ and - - - for sway-referenced vision). For the eyes closed condition, w_p was very close to 1 for all stimulus amplitudes tested (mean $w_p = 0.995$). Therefore $w_g = 1 - w_p$ was nearly zero. This result suggests that the source of sensory information used for postural control was derived entirely from proprioceptive receptors in this condition and that graviceptor information did not contribute to postural control. Because this was a VL subject, the absence of a graviceptor contribution also implies that vestibular sensors were the entire source of this subject's graviceptor information used for postural control in this condition. However, unlike normal subjects, the results from the sway-referenced condition were not quite the same as from the eyes closed condition. In this case, w_p was slightly less than 1 at all stimulus amplitudes (mean $w_p = 0.88$), and w_g was therefore equal to 0.12, suggesting that this subject had some access to graviceptive information in this condition. Alternatively, one could speculate that this subject was able to derive some useful information from visual cues (possibly due to imperfections in sway-referencing of the visual surround). A similar discrepancy between eyes closed and sway-referenced vision results also occurred with *subjects VL1* and *VL3,* with w_p values determined from the sway-referenced condition being lower than from the eyes closed condition. *Subject VL4* was unable to complete any trial with a sway-referenced visual surround even though she was able to perform tests with eyes closed.

Figure 14, *bottom,* shows the results derived from three different test conditions. In each of these test conditions, we anticipated that visual, proprioceptive, and graviceptive information would all be contributing to postural control. The w_v results were derived from tests with visual stimulation on a fixed support surface. In this condition, $w_v = W = 1 - w_p - w_g$. The w_p results were derived from tests with support surface stimulation and a fixed visual surround. In this condition, $w_p = W = 1 - w_v - w_g$. Once w_v and w_p were known, w_g was calculated $w_g = 1 - w_v - w_p$. The results for normal subjects are shown in the *three lower row plots* in Fig. 14 ($\bullet$ and —). The calculation of w_g in this case depended on the possibly invalid assumption that w_v and w_p values obtained at a given stimulus amplitude in two different test conditions were comparable. An approximate check on this assumption was provided by results from the test condition with combined support surface and visual surround stimulation. In this condition, $W = w_v + w_p$, and therefore $w_g = 1 - W$. Results for normal subjects of this w_g calculation, plotted in the lower right graph of Fig. 14 ($\circ$ with - - -), show a close, but not exact, correspondence to the w_g values derived from the two separate test conditions.

The results for normal subjects shown in Fig. 14, *bottom,* demonstrate that in conditions where two of the three sensory channels were providing veridical orientation cues, the visual channel contribution to postural control was always smaller than the proprioceptive channel contribution. The average difference between w_p and w_v across all stimulus amplitudes was 0.17. With increasing stimulus amplitudes, the contribution of both visual and proprioceptive channels decreased and the graviceptive channel showed a corresponding increase. At the highest stimulus amplitude tested, the graviceptive channel contribution dominated, and there was essentially no contribution from the visual channel ($w_g = 0.82$, $w_p = 0.15$, $w_v = 0.03$).

Results for two example VL subjects derived from test conditions with the visual surround fixed, support surface fixed, or combined visual and support surface stimulation, are also plotted in Fig. 14 (*bottom,* $\triangle$, $\blacktriangle$ and $\times$). These results were derived in the same manner as the results from the normal subjects. In one of the VL subjects (*VL2,* $\blacktriangle$ and — for results derived from fixed visual surround or fixed support surface conditions), w_p was always larger than w_v, and there was only a small decline in these sensory channel weights with increas-

ing stimulus amplitude. The graviceptive channel contribution was close to zero except at the highest stimulus amplitude tested (4°). The w_g values derived from the combined stimulus conditions ($\triangle$, $\cdots$) were similar to w_g values derived from test conditions with either the visual surround or the support surface fixed and showed that there was essentially no graviceptive contribution to postural control in this subject with absent vestibular function. The results from two of the other VL subjects (*VL1* and *VL4*) were similar to this subject with the exception that w_v and w_p were approximately equal in these two subjects. *Subject VL3,* who had the most preserved vestibular function (Table 1), showed a different behavior. His results are also plotted in Fig. 14 (*bottom,* $\times$ with — for results derived from conditions with fixed surround or support surface and $\cdots$ for results derived from combined stimulation). This subject showed a visual channel contribution of $w_v = 0.4$ that was independent of the stimulus amplitude. However, w_p declined with increasing stimulus amplitude. The overall result was that w_g was zero for the 1° stimulus condition but increased to a value of about 0.2 at the 4° stimulus condition. The w_g values from the combined stimulus condition were in close agreement with those derived from the separate test conditions.

DISCUSSION

Human postural control behavior over a bandwidth of 0.017–2.23 Hz was characterized by applying pseudorandom support surface and/or visual perturbations of varying amplitudes and interpreting responses based on a simple negative feedback model (Fig. 9). Subjects tended to align their body to the perturbing stimulus such that the general waveform of the body-sway angle response was similar to the stimulus waveform (Fig. 3). As the stimulus amplitude was increased, the body-sway response initially increased but then saturated for peak-to-peak stimulus amplitudes greater than about 2° for subjects with normal vestibular function (Fig. 4, ● and —). For subjects with bilaterally absent vestibular function, responses continued to increase with increasing stimulus amplitude (Fig. 4, $\cdots$).

The stimulus-response waveforms were analyzed using Fourier methods to calculate gain, phase, and coherence measures as a function of stimulus frequency (Figs. 5–8). A gain of unity and phase of zero indicates that the subject remained perfectly aligned to the stimulus in amplitude (e.g., body-sway angle equals support surface or visual surround tilt angle) and time (i.e., no time delay or advance of body sway relative to the stimulus). Such perfect alignment was never achieved. Phase measures typically showed a phase lead at frequencies less than about 0.1 Hz. Phase functions crossed zero in the 0.1–0.2 Hz range, increased with increasing frequency, and reached lags as high as 350–400° at 2.23 Hz (Fig. 6).

The large and increasing phase lags with increasing frequency are consistent with the existence of a significant time delay between the stimulus and the resulting body-sway response. This time delay was present in responses to both visual and support surface stimuli. The existence of a large time delay seems incompatible with the possibility that stabilizing torque might be obtained primarily via passive mechanisms as suggested previously (Winter et al. 1998, 2001) because passive stiffness mechanisms should act without time delay. Also, our estimates of passive stiffness and damping parameters obtained

from curve fits of *Eq. 15* to experimental transfer function data showed these passive factors to be about 1/10th the value of active stiffness and damping parameters.

Explanation of response dynamics

Gain functions were maximal between about 0.1–0.5 Hz for both normal (Fig. 6) and VL subjects (Fig. 8). For frequencies greater than 0.5 Hz, gains monotonically declined with increasing frequency. The peak gain values were often greater than unity, particularly for low-amplitude stimuli where mean gains as large as 4.1 were obtained (mean normal gain for 0.5° visual stimulus on sway-referenced surface). Gain values greater than unity indicate that the amplitude of stimulus-evoked body sway was greater than the stimulus amplitude.

Gain values greater than unity may seem to be an unlikely result. However, large gains have been demonstrated previously (Gurfinkel et al. 1995; Lee and Lishman 1975; Peterka and Benolken 1995) in response to low-amplitude stimuli. Large gains are also consistent with postural regulation via a negative feedback control mechanism where, in steady state, corrective torque is generated in proportion to a position error signal. This is easiest to see if one considers a postural control system consisting of only one sensory system. Consider, for example, a system with only proprioceptors, which signal body orientation relative to the support surface (Fig. 9 with $w_v = w_g = 0$, $w_p = 1$). In this system, an error signal, indicating body sway relative to the support surface, is used to generate a corrective torque that changes the body-sway angle in space and reduces the error signal. If this control system could maintain zero error, then the body would remain oriented to the support surface, and the transfer function gain would be unity across all stimulus frequencies. However, a control system typically will not be able to achieve a zero error condition. The error depends on the system's overall properties that include body and neural controller dynamics. To see that gains can be greater than unity, consider a simplified neural controller that does not include the integral control factor, K_I (integral control mainly affects very low-frequency dynamics). In this system, the steady-state gain is predicted to be $K_P/(K_P - mgh)$. This result is obtained from *Eq. 14* by setting $W = 1$, $K_I = 0$ and setting the Laplace variable $s = 0$ [see Peterka and Benolken (1995) and also a similar derivation in Gurfinkel et al. (1995)]. Because the gravity-related factor mgh is a positive value, the predicted gain is greater than unity, and the gain value tells us about the size of K_P relative to mgh. Qualitatively, this result means that when the support surface tilts, a steady-state body-sway angle is reached that represents the equilibrium point where the torque due to gravity, $mgh \sin(BS)$, is balanced by the compensatory torque generated by the neural controller, $K_P(FS - BS)$. At this equilibrium point, the body-sway angle from vertical will always be greater than the tilt angle of the support surface, and therefore the gain is greater than unity.

Experimental results show that the highest gains typically occur in the 0.1–0.2 Hz frequency range where the response phases are also closest to zero. It is reasonable to assume that responses in this mid-frequency region are dominated by the stiffness component of the neural controller and its interaction with the spring-like torque due to gravity. Body motions at these frequencies are slow enough that there is time for the

body to reach an equilibrium position that reflects the torque balance between neural controller and gravity torques.

At higher frequencies, the body-sway response becomes increasingly dominated by inertial torques, which tend to keep the body fixed in space (gains approach 0) and therefore resist orientation toward the stimulus. The interplay between inertial torque and active torque due to stiffness and damping components of the neural controller would result in response phases approaching $-90°$ at higher frequencies, if there was no time delay in the system. With the addition of time delay, phase lags continue to increase with increasing frequency, consistent with the experimental data. The inclusion of a time delay in the model was able to account for much of the phase lag at higher frequencies (e.g., Fig. 5, *C* and *D*). However, even with the inclusion of a time delay, the transfer function fit (*Eq. 14*) was not always able to account for all of the phase lag in the experimental data (e.g., Figs. 5, *A* and *B*, and 8*D*). This poor fit to the higher-frequency data was more common for data obtained in response to 0.5 or 1° stimuli (Fig. 5, *A* and *B*) than for data from higher-amplitude stimuli (Fig. 5, *C* and *D*). Failure of the independent channel model to fully explain the higher-frequency data indicates that this model is not accounting for all of the factors that contribute to dynamic behavior greater than about 1.2 Hz. These factors might include low-pass dynamics in the sensory channels and muscle mechanics that have low-pass characteristics (Zajac 1989).

At frequencies lower than about 0.1 Hz, experimental results show gain declines and phase advances. This dynamic behavior cannot be explained if corrective torque is only generated in proportion to body position and velocity relative to the support surface (FS − BS). In a system with only one sensor signaling orientation with respect to the support surface, this low-frequency dynamic behavior necessarily requires that corrective torque be generated as some function of body orientation that emphasizes low frequencies. One possibility is that a component of corrective torque is generated in proportion to the time integral of the error signal FS − BS as represented by the K_I factor in the neural controller in Fig. 9. The inclusion of an integral control component has been previously suggested to explain the dynamic properties of vibration-evoked body sway (Johansson et al. 1988). In this previous study, the normalized integral control parameter was referred to as a "swiftness" factor. Alternatively, low-frequency gain declines could be produced by a contribution from an additional sensory cue that only influenced low-frequency behavior and was opposed to the sensory cue that encoded body sway relative to the stimulus. For example, if the corrective torque included a contribution from a sensory system conveying low-frequency graviceptive information, then low-frequency behavior might be dominated by the graviceptive cue producing orientation toward earth-vertical, while mid-frequency behavior is dominated by proprioceptive and/or visual cues that produce orientation to the support surface and/or visual surround.

For a one sensor system, the use of integral control would only be able to reduce the low-frequency gain to unity. This prediction seems compatible with the gain data from some VL subjects tested in conditions that limited either visual or support surface cues (e.g., Fig. 8, *A* and *D*). However, the observed low-frequency phase data from both normal subjects and VL subjects were not always fully explained by the addition of an integral control factor. Specifically, the phase data often showed significant phase leads at frequencies less than about 0.1 Hz (Figs. 5, 6, and 8). Inclusion of a K_I factor in the neural controller was only able to account for some of this phase lead. In a model transfer function that includes a K_I factor (*Eq. 14*), the maximum phase advance will always be less than 90°, and the phase will approach zero at very low frequencies. However, the average normal phase data in Fig. 5 showed that there was little or no tendency for the phase lead to decline toward zero with decreasing frequency, and the experimentally measured phase often showed a larger phase lead than could be explained by the model. The model's phase behavior and the disparity between the low-frequency model and experimental phase data can be clearly seen in Figs. 5, *B* and *C*, and 8*D*. Therefore, inclusion of a K_I factor in the model neural controller did not provide a full explanation of the low-frequency behavior of the postural control system.

Interpretation of response saturation

In subjects with normal sensory function, responses to increasing amplitudes of visual or support surface stimuli showed saturation behavior (Fig. 4). One might speculate that this is the result of some nonlinear processing of sensorimotor signals that limit the responses to larger amplitude stimuli. If this were the case, then one would expect that coherence functions should show some evidence for increasingly nonlinear stimulus-response behavior with increasing stimulus amplitude. That is, with perfectly linear stimulus-response behavior in the absence of noise, the coherence function will be unity across all test frequencies. The presence of noise and/or nonlinear behavior results in a decrease in coherence function values. If increasing stimulus amplitudes drove the system further into some type of saturating nonlinearity, one would expect to see decreases in coherence function values with increasing stimulus amplitude. This was not observed. At stimulus amplitudes of 1° and above, there was no obvious decrease in coherence function values with increasing stimulus amplitude that might indicate the influence of a saturating nonlinearity. Note that decreases in coherence function values do not necessarily occur when a nonlinearity is present (Maki 1986). However, simulation results using our specific PRTS stimulus applied to a system with a saturating nonlinearity did show decreased coherence function values with increasing stimulus amplitude.

The similar coherence function values suggest that stimulus-response behavior was as linear in the 1° stimulus condition as in the 8° condition even though gain functions differed greatly between these two stimulus conditions, indicating overall nonlinear behavior of the system. This apparent contradiction can be explained if one assumes that sensory weighting factors changed as a function of stimulus amplitude, thereby providing quasi-linear behavior at each stimulus amplitude. The large decrease in gain can occur if the predominant sensory contribution shifts from the proprioceptive and/or visual system to a graviceptive system with increasing stimulus amplitude.

The absence of some fundamental saturating nonlinearity in the postural control system is further supported by the results from VL subjects. These subjects did not show saturating behavior (Fig. 4, · · ·), and transfer function results showed very limited changes in gain with stimulus amplitude. However, their coherence function results were nearly the same as

those in normal subjects (e.g., Fig. 8*A*). From this observation in VL subjects, we can postulate that both the interaction of proprioceptive and visual orientation cues, and the overall behavior of the motor output system are essentially linear. If this essentially linear proprioceptive/visual interaction is also true for subjects with normal sensory function, then the overall nonlinear behavior to changing stimulus amplitude must involve a nonlinear interaction of vestibular cues with proprioceptive/visual cues. One likely possibility is that this nonlinear interaction is representative of a sensory selection mechanism that alters the relative contribution of different sensory orientation cues in different conditions. This effect can be functionally characterized as a stimulus-dependent reweighting of sensory channels. Our results showed that the variation in channel weights among normal subjects for any given stimulus amplitude and condition was very small (see SD error bars in Fig. 14), indicating that all of our normal subjects used nearly identical selection strategies for a given condition and amplitude.

A recent adaptive model of sensory integration for human postural control has been proposed based on optimal estimation theory (van der Kooij et al. 2001). This model was able to predict the amplitude-dependence of body sway evoked by sinusoidal visual surround rotations for both normal and VL subjects (Peterka and Benolken 1995). These previous data are qualitatively similar to the PRTS responses reported here, showing response saturation in normal but not in VL subjects. Therefore it appears that this new adaptive model provides a basis for interpreting sensory reweighting in terms of the goals and limitations of the sensorimotor integration process as it applies to postural control.

Optimal estimation models also provide a basis for understanding how the nervous system might transform raw sensory signals into internal estimates of body motion and spatial orientation (Merfeld 1995; van der Kooij et al. 1999; Zupan et al. 2002). Although our simple model (Fig. 9) does not include mechanisms for optimal estimation of body motion, it does assume that wide bandwidth motion information is available to the postural control system. Complex sensory integration processes represented by optimal estimation models likely are necessary to provide the wide bandwidth motion information used in postural control.

Sensory channel reweighting and "torque normalization"

Consider a test condition where only two modalities are available for balance control in normal subjects. Specifically, consider support surface stimulation with eyes closed, where proprioceptive and graviceptive cues contribute to balance control. The observed decrease in transfer function gain with increasing support surface amplitude implies that a relative reduction in responsiveness to proprioceptive cues occurs with increasing stimulus amplitude. This relative reduction in responsiveness can be expressed as a decrease in the proprioceptive channel weight, w_p, with increasing stimulus amplitude. In a closed-loop control system, a reduction of a gain factor inside a feedback loop can severely affect dynamic behavior. In the Fig. 9 model, a reduction in w_p alone causes the overall transfer function to develop resonant properties as the level of net corrective torque decreases. If w_p is so low that the corrective torque is insufficient to resist the torque due to gravity, the

system becomes unstable. The fact that the transfer function dynamics do not change greatly with changing stimulus amplitude (Fig. 6) implies that the net corrective torque does not change greatly with decreasing w_p. This indirectly implies that another signal contributing to torque generation increases as w_p decreases. A reasonable assumption consistent with the experimental data and embodied in the Fig. 9 model is that the graviceptive contribution (represented by w_g) to net torque generation increases as the proprioceptive contribution decreases. The same argument applies for the condition where only visual and graviceptive cues contribute to balance control (visual stimulation on sway-referenced support surface). In this case, w_g increases as w_v decreases.

Therefore the modeling assumption that the sum of sensory channel weights is unity is essentially a "torque normalization" hypothesis. This hypothesis implies that some mechanism exists that ensures that an appropriate level of corrective torque is generated to not only maintain stance but to maintain good (i.e., nonresonant) dynamic behavior independent of the particular source of sensory cues that are contributing to torque generation in a particular environmental condition. Complete adherence to a torque normalization principle would imply that the shapes of the transfer functions never change even though the overall contribution of individual sensory channels changes with varying stimulus conditions. It is likely that torque normalization is not always perfectly maintained, and this could account for the relatively rare occurrences where resonant transfer function dynamics were observed. For example, the Fig. 5*B* transfer function with a resonant peak at about 0.2 Hz is consistent with there being too little corrective torque generated in proportion to body sway, and the Fig. 5*C* transfer function showing a 0.9 Hz resonance peak is consistent with there being too much corrective torque.

Sensory channel weighting in VL subjects

For VL subjects tested in the three conditions that limited sensory orientation cues from one modality (either vision or proprioception) or in the one condition that provided an identical stimulus to both the visual and proprioceptive systems, the prediction of the independent channel model (Fig. 9) is that the identified sensory weighting factor, *W*, should be unity if all of the graviceptive information used for postural control were derived from the vestibular system. To a good approximation, this was true for all four VL subjects (Fig. 10, VL results in *top row*). The small deviations from this prediction might be accounted for by various experimental imperfections including misestimates of body moment of inertia and COM height used in the curve fit procedures, imperfections in sway-referencing, the fact that vestibular function may not be entirely absent in these subjects, and the possibility that VL subjects may compensate for their loss by making some small use of nonvestibular graviceptive information (Mittelstaedt 1998).

Another clear difference between normal and VL subjects was evident in test conditions where either the visual surround or the support surface was fixed. In normal subjects, the value of *W* decreased with increasing stimulus amplitude (Fig. 10, *bottom 2 curves* in *top left plot*), indicating that there was a decrease in responsiveness to the stimulus with increasing amplitude and indirectly implying a decrease in w_p or w_v channel weights. In contrast, VL subjects showed a more

limited ability, and in some cases, no ability (e.g., *VL2* in Fig. 14, *bottom*) to modify w_p and w_v with increasing stimulus amplitude. If only two sensory modalities contribute to postural control and neither of these modalities provide absolute earth-referenced information, then a reasonable strategy may simply be to generate corrective torque as a fixed combination of signals from these two modalities independent of the stimulus amplitude and without attempting to make a decision about which of the two sensory systems might possibly be providing veridical orientation information.

In conditions where both visual and proprioceptive cues were available, three of the four VL subjects showed little ability to alter the visual and proprioceptive channel weights with varying stimulus amplitude as indicated by the limited changes in *W* (Fig. 10, VL results in *top row, bottom 2 traces* in each plot). One subject, *VL3,* could markedly decrease his proprioceptive channel weight with increasing support surface rotation (fixed visual surround condition). Given that other test conditions showed that this subject was unable to utilize graviceptive cues for postural control, this decreased proprioceptive weight was likely associated with an increased visual channel weight. That is, over the course of our relatively long duration tests, this subject may have been able to determine that visual cues were providing veridical orientation information and therefore relied more heavily on them. One could imagine trial and error changes in sensory channel weights occurring with the effectiveness of the weight change judged by monitoring the muscular effort necessary to maintain balance. One could also imagine that in a richer sensory environment than that afforded by our test apparatus, cognitive factors based on prior knowledge of the stability of the visual world or surface condition could influence sensory channel weight selection.

Compensation for bilateral VL

All of the VL subjects received their loss several years prior to our testing, and would clinically be considered well compensated. (One possible exception would be *subject VL4,* who showed visual preference behavior.) An interesting question is whether or not there was evidence for sensory substitution for their vestibular loss. For example, there is evidence that subjects have access to graviceptive cues that are not of vestibular origin (Mittelstaedt 1998). Perhaps these could be substituted for missing vestibular cues. Our results show little evidence that some other nonvestibular graviceptive source was utilized by our VL subjects. When VL subjects were tested under conditions that eliminated or greatly limited visual or proprioceptive orientation cues (by eye closure or sway-referencing of the visual surround or by support surface sway-referencing), the sensory weighting factor, *W*, identified from our transfer function fits was very close to unity and varied little with changing stimulus amplitudes (Fig. 10, *top*). By our interpretation, a unity value of *W* in these conditions indicates that VL subjects were deriving all of their orientation information from one source, either vision or proprioception.

There was evidence some VL subjects used an increase in stiffness to compensate for their vestibular loss. Among all of the normal and VL subjects tested, the two subjects with the greatest relative stiffness (K_P normalized for body moment of inertia) on low-amplitude tests were both VL subjects (Fig. 13, *left*). As discussed previously, maintenance of a relatively high stiffness could provide a compensatory strategy which reduces the sensory error signal ("*e* " in Fig. 9), and thereby enhances orientation toward the available sensory reference. As is appropriate to maintain nonresonant dynamics, the increase in K_P in these two subjects was accompanied by both a relative increase in K_D and decrease in τ_d to provide for increased damping.

A compensation strategy that uses increased stiffness necessarily requires an increased energy expenditure. Perhaps this is the reason that the other two VL subjects did not adopt a strategy of increased stiffness. In fact, one of the VL subjects had the second lowest relative stiffness among all subjects tested.

Changes in apparent feedback time delay

There was a consistent difference between the family of phase functions obtained from visual stimuli and those obtained from support surface stimuli (Fig. 6). For visual stimuli, the phase functions at frequencies greater than about 0.2 Hz were nearly identical for all stimulus amplitudes. In contrast, for support surface stimuli, the phase functions greater than 0.2 Hz showed less phase lag with increasing stimulus amplitude. A reduced phase lag could be consistent with a smaller time delay (this is the interpretation based on curve fits of *Eq. 14* derived from the independent channel model). However, other mechanisms that might explain this phenomenon are considered in the following text.

One might speculate that a shorter time delay could result from an increased contribution of a sensory system that acts with a shorter time delay (i.e., there might be a shorter time delay in the vestibular contribution to corrective torque generation compared with the proprioceptive time delay). Alternatively, if there was an increased contribution of corrective torque due to "passive" muscle/tendon properties (which act with zero time delay) compared with active torque generation, then the time delay might appear to decrease. However, preliminary results from recent experiments using a time domain analysis of responses to high bandwidth PRTS stimuli suggest that the actual time delay does not change with stimulus amplitude (Peterka 2001). These results favor the existence of a mechanism that compensates for time delay without changing the actual time delay or changing the active versus passive contributions to torque generation. Such a mechanism is not included in the independent channel model but has been suggested in other postural control models (Morasso et al. 1999; van der Kooij et al. 1999, 2001) and in motor systems in general (Kleinman et al. 1970; Miall et al. 1993). Therefore the time delay parameter, τ_d, in the independent channel model should be thought of as an "effective time delay" rather than as a parameter representing actual delays in neural processing, transmission, and muscle activation.

If a mechanism for time delay compensation exists, why does it exist? When the independent channel model is simulated, it becomes easy to appreciate that an increase in the active stiffness parameter K_P by 60% (as shown in Fig. 10 for increasing support surface stimulus amplitudes with fixed visual surround) causes a 1 Hz resonant peak to develop in the transfer function indicating that the system is close to instability. However, experimental data never showed a 1 Hz resonant peak because this stiffness increase was apparently accompanied by an appropriate increase in overall damping. There are

two ways to increase damping, the most obvious of which is to increase K_D, but a decrease in τ_d has a nearly identical effect. Our results showed that there was a small increase in K_D in conditions where K_P increased (Fig. 10, *left*), but a larger portion of the overall damping increase was accomplished by a decrease in the effective time delay. Additionally, Fig. 11*A* shows a strong correlation between τ_d and K_P. We suggest that a relationship exists between τ_d and K_P because changes in the effective time delay are the primary method used by the postural control system to regulate the overall damping to compensate for changes in stiffness in different test conditions.

Is feedback control sufficient?

Our general conclusion is that a feedback control mechanism is sufficient to account for postural control behavior over a wide bandwidth. This was not the conclusion reached previously (Fitzpatrick et al. 1996), where it was postulated that feedforward predictive control mechanisms were required. We suggest that Fitzpatrick's well-reasoned attempt to break open and test individual components of the feedback system was confounded by the postural control system's ability to reweight sensory information in different test conditions. Specifically, this unanticipated reweighting resulted in an underestimation of the overall sensory contribution to feedback control in this previous study.

The results of stabilogram-diffusion analysis of quiet stance COP data have been used to infer the existence of both "open loop" and "closed loop" control of posture (Collins and De Luca 1993). However, recent results have shown that stabilogram-diffusion functions obtained from simulations using a feedback model like the one in Fig. 9 are indistinguishable from experimental stabilogram-diffusion functions (Peterka 2000), thus demonstrating that feedback control mechanisms alone are sufficient to explain the shape of stabilogram-diffusion functions obtained from experimental COP data.

We find further support for a feedback control scheme that relies on actively generated corrective torque and sensory reweighting because it appears compatible with a number of pathological conditions. For example, this model predicts and is consistent with experimental results (Nashner et al. 1982) that stance is impossible for VL subjects deprived of visual cues (eye closure) and veridical proprioceptive cues (support surface sway-referencing). However, stance is possible, and even potentially indistinguishable from normal, if VL subjects have either veridical visual or proprioceptive cues (Black et al. 1983). A number of pathological postural behaviors are also compatible with failure of feedback regulation, resulting in an underproduction of corrective torque. Specifically, patterns of behavior revealed on clinical sensory organization tests referred to as "visual preference", "somatosensory dependent" (also called "visual and vestibular dysfunction"), or "vision dependent" (Nashner 1993b) could potentially result from a failure of sensory reweighting and/or torque normalization. Similarly, normal subjects initially show diminished responses to surface perturbations when the visual surround is sway-referenced, but responses return to normal with repeated stimulus presentations (Nashner 1982). Because normal subjects typically derive about one-third of their orientation information from vision during eyes-open quiet stance (Fig. 14, *bottom left graph*), initial exposure to a sway-referenced visual condition, where VB = 0 in the Fig. 9 model, results in a reduced generation of corrective torque. With repeated stimulus presentations, torque normalization occurs such that $w_p + w_v = 1$, and responses return to normal levels. Finally, a failure of feedback regulation that results in an overproduction of corrective torque is predicted by the Fig. 9 model to produce 1–3 Hz oscillatory behavior (depending on whether K_P, K_D, or both are greater than normal). Such behavior has been seen in subjects with cerebellar deficits (Dichgans et al. 1976; Diener and Dichgans 1992; Diener et al. 1984a), in normal subjects with experimentally applied leg ischemia (Diener et al. 1984c; Mauritz and Dietz 1980), and following environmental transitions that suddenly increase access to accurate sensory orientation cues (Peterka and Loughlin 2002).

REFERENCES

ALLUM JHJ. Organization of stabilizing reflex responses in tibialis anterior muscles following ankle flexion perturbations of standing man. *Brain Res* 264: 297–301, 1983.

BENDAT JS AND PIERSOL AG. *Random Data: Analysis and Measurement Procedures*. New York: Wiley, 2000.

BERTHOZ A, LACOUR M, SOECHTING JF, AND VIDAL PP. The role of vision in the control of posture during linear motion. *Prog Brain Res* 50: 197–210, 1979.

BLACK FO, WALL C III, AND NASHNER LM. Effects of visual and support surface orientation references upon postural control in vestibular deficient subjects. *Acta Otolaryngol (Stockh)* 95: 199–210, 1983.

BRENIÈRE Y. Why we walk the way we do. *J Mot Behav* 28: 291–298, 1996.

BRITTON TC, DAY BL, BROWN P, ROTHWELL JC, THOMPSON PD, AND MARSDEN CD. Postural electromyographic responses in the arm and leg following galvanic vestibular stimulation in man. *Exp Brain Res* 94: 143–151, 1993.

BRONSTEIN AM. Suppression of visually evoked postural responses. *Exp Brain Res* 63: 665–658, 1986.

COLLINS JJ AND DE LUCA CJ. Open-loop and closed-loop control of posture: a random-walk analysis of center-of-pressure trajectories. *Exp Brain Res* 95: 308–318, 1993.

DAVIES WDT. *System Identification for Self-Adaptive Control*. London, UK: Wiley-Interscience, 1970.

DAY BL, SEVERAC CAUQUIL A, BARTOLOMEI L, PASTOR MA, AND LYON IN. Human body-segment tilts induced by galvanic stimulation: a vestibularly driven balance protection mechanism. *J Physiol (Lond)* 500: 661–672, 1997.

DICHGANS J, MAURITZ KH, ALLUM JHJ, AND BRANDT T. Postural sway in normals and atactic patients: analysis of the stabilizing and destabilizing effect of vision. *Agressologie* 17C: 15–24, 1976.

DIENER HC AND DICHGANS J. Pathophysiology of cerebellar ataxia. *Mov Disord* 7: 95–109, 1992.

DIENER HC, DICHGANS J, BACHER M, AND GOMPF B. Quantification of postural sway in normals and patients with cerebellar diseases. *Electroencephalogr Clin Neurophysiol* 57: 134–142, 1984a.

DIENER HC, DICHGANS J, BOOTZ F, AND BACHER M. Early stabilization of human posture after a sudden disturbance: influence of rate and amplitude of displacement. *Exp Brain Res* 56: 126–134, 1984b.

DIENER HC, DICHGANS J, GUSCHLBAUER B, AND MAU H. The significance of proprioception on postural stabilization as assessed by ischemia. *Brain Res* 296: 103–109, 1984c.

DIJKSTRA TMH, SCHÖNER G, AND GIELEN CCAM. Temporal stability of the action-perception cycle for postural control in a moving visual environment. *Exp Brain Res* 97: 477–486, 1994a.

DIJKSTRA TMH, SCHÖNER G, GIESE MA, AND GIELEN CCAM. Frequency dependence of the action-perception cycle for postural control in a moving visual environment: relative phase dynamics. *Biol Cybern* 71: 489–501, 1994b.

FITZPATRICK R, BURKE D, AND GANDEVIA SC. Task-dependent reflex responses and movement illusions evoked by galvanic vestibular stimulation in standing humans. *J Physiol (Lond)* 478: 363–372, 1994.

FITZPATRICK R, BURKE D, AND GANDEVIA SC. Loop gain of reflexes controlling human standing measured with the use of postural and vestibular disturbances. *J Neurophysiol* 76: 3994–4008, 1996.

FORSSBERG H AND NASHNER LM. Ontogenetic development of postural control in man: adaptation to altered support and visual conditions during stance. *J Neurosci* 2: 545–552, 1982.

GURFINKEL VS, IVANENKO YP, LEVIK YS, AND BABAKOVA IA. Kinesthetic reference for human orthograde posture. *Neuroscience* 68: 229–243, 1995.

HAJOS A AND KIRCHNER W. Körperlageregelung des Menschen bei elekrischer Reizung des Vestibularsystems. In: *Sensory Experience, Adaptation, and Perception*, edited by Spillmann L and Wooten BR. London: Erlbaum, 1984, p. 255–280.

HLAVACKA F AND NIJIOKIKTJIEN C. Postural responses evoked by sinusoidal galvanic stimulation of the labyrinth. *Acta Otolaryngol (Stockh)* 99: 107–112, 1985.

HORAK FB AND MACPHERSON JM. Postural orientation and equilibrium. In: *Handbook of Physiology. Exercise: Regulation and Integration of Multiple Systems*, edited by Rowell LB and Shepherd JT. New York: Oxford, 1996, sect. 12, p. 255–292.

HORAK FB AND NASHNER LM. Central programming of postural movements: adaptation to altered support-surface configurations. *J Neurophysiol* 55: 1369–1381, 1986.

HULTBORN H. State-dependent modulation of sensory feedback. *J Physiol (Lond)* 533: 5–13, 2001.

ISHIDA A AND IMAI S. Analysis of the sensory information of postural regulation utilizing a servo-controlled force plate. *Agressologie* 24: 61–62, 1983.

JEKA J, OIE KS, AND KIEMEL T. Multisensory information for human postural control: integrating touch and vision. *Exp Brain Res* 134: 107–125, 2000.

JEKA J, OIE K, SCHÖNER G, DIJKSTRA T, AND HENSON E. Position and velocity coupling of postural sway to somatosensory drive. *J Neurophysiol* 79: 1661–1674, 1998.

JEKA JJ, SCHÖNER G, DIJKSTRA T, RIBEIRO P, AND LACKNER JR. Coupling of fingertip somatosensory information to head and body sway. *Exp Brain Res* 113: 475–483, 1997.

JOHANSSON R AND MAGNUSSON M. Human postural dynamics. *Biomed Eng* 18: 413–437, 1991.

JOHANSSON R, MAGNUSSON M, AND AKESSON M. Identification of human postural dynamics. *IEEE Trans Biomed Eng* 35: 858–869, 1988.

JOHANSSON R, MAGNUSSON M, AND FRANSSON PA. Galvanic vestibular stimulation for analysis of postural adaptation and stability. *IEEE Trans Biomed Eng* 42: 282–292, 1995.

KAVOUNOUDIAS A, GILHODES JC, ROLL R, AND ROLL JP. From balance regulation to body orientation: two goals for muscle proprioceptive information processing? *Exp Brain Res* 124: 80–88, 1999.

KESHNER EA, HAIN TC, AND CHEN KJ. Predicting control mechanisms for human head stabilization by altering the passive mechanics. *J Vestib Res* 9: 423–434, 1999.

KLEINMAN DL, BARON S, AND LEVISON WH. An optimal control model of human response. I. Theory and validation. *Automatica* 6: 357–369, 1970.

LEE DN AND LISHMAN JR. Visual proprioceptive control of stance. *J Hum Move Studies* 1: 87–95, 1975.

LESTIENNE F, SOECHTING J, AND BERTHOZ A. Postural readjustments induced by linear motion of visual scenes. *Exp Brain Res* 28: 363–384, 1977.

MAKI BE. Interpretation of the coherence function when using pseudorandom inputs to identify nonlinear systems. *IEEE Trans Biomed Eng* BME-33: 775–779, 1986.

MAKI BE, HOLLIDAY PJ, AND FERNIE GR. A posture control model and balance test for the prediction of relative postural stability. *IEEE Trans Biomed Eng* 34: 797–810, 1987.

MAURITZ KH AND DIETZ V. Characteristics of postural instability induced by ischemic blocking of leg afferents. *Exp Brain Res* 38: 117–119, 1980.

MCILROY WE AND MAKI BE. The "deceleration response" to transient perturbation of upright stance. *Neurosci Lett* 175: 13–16, 1994.

MERFELD DM. Modeling the vestibulo-ocular reflex of the squirrel monkey during eccentric rotation and roll tilt. *Exp Brain Res* 106: 123–134, 1995.

MERGNER T, HUBER W, AND BECKER W. Vestibular-neck interaction and transformation of sensory coordinates. *J Vestib Res* 7: 347–367, 1997.

MERGNER T, SIEBOLD C, SCHWEIGART G, AND BECKER W. Human perception of horizontal trunk and head rotation in space during vestibular and neck stimulation. *Exp Brain Res* 85: 389–404, 1991.

MIALL RC, WEIR DJ, WOLPERT DM, AND STEIN JF. Is the cerebellum a Smith predictor? *J Mot Behav* 25: 203–216, 1993.

MITTELSTAEDT H. Origin and processing of postural information. *Neurosci Biobehav Rev* 22: 473–478, 1998.

MORASSO PG, BARATTO L, CAPRA R, AND SPADA G. Internal models in the control of posture. *Neural Networks* 12: 1173–1180, 1999.

MORASSO PG AND SCHIEPPATI M. Can muscle stiffness alone stabilize upright standing? *J Neurophysiol* 82: 1622–1626, 1999.

NASHNER LM. Fixed patterns of rapid postural responses among leg muscles during stance. *Exp Brain Res* 30: 13–24, 1977.

NASHNER LM. Adaptation of human movement to altered environments. *Trends Neurosci* 5: 358–361, 1982.

NASHNER LM. Computerized dynamic posturography. In: *Handbook of Balance Function Testing*, edited by Jacobson GP, Newman CW, and Kartush JM. St. Louis, MO: Mosby-Year Book, 1993a, p. 280–307.

NASHNER LM. Computerized dynamic posturography: clinical applications. In: *Handbook of Balance Function Testing*, edited by Jacobson GP, Newman CW, and Kartush JM. St. Louis, MO: Mosby-Year Book, 1993b, p. 308–334.

NASHNER LM AND BERTHOZ A. Visual contribution to rapid motor responses during posture control. *Brain Res* 150: 403–407, 1978.

NASHNER LM, BLACK FO, AND WALL C III. Adaptation to altered support and visual conditions during stance: patients with vestibular deficits. *J Neurosci* 2: 536–544, 1982.

NASHNER LM AND WOLFSON P. Influence of head position and proprioceptive cues on short latency postural reflexes evoked by galvanic stimulation of the human labyrinth. *Brain Res* 67: 255–268, 1974.

OTNES RK AND ENOCHSON L. *Digital Time Series Analysis*. New York: Wiley, 1972.

PETERKA RJ. Postural control model interpretation of stabilogram diffusion analysis. *Biol Cybern* 82: 335–343, 2000.

PETERKA RJ. Compensation for reflex time delay in the human postural control system (Abstract). *Neural Control Move* 6: B-06, 2001.

PETERKA RJ AND BENOLKEN MS. Role of somatosensory and vestibular cues in attenuating visually induced human postural sway. *Exp Brain Res* 105: 101–110, 1995.

PETERKA RJ AND BLACK FO. Age-related changes in human posture control: sensory organization tests. *J Vestib Res* 1: 73–85, 1990.

PETERKA RJ, BLACK FO, AND SCHOENHOFF MB. Age-related changes in human vestibulo-ocular reflexes: sinusoidal rotation and caloric tests. *J Vestib Res* 1: 49–59, 1990.

PETERKA RJ AND LOUGHLIN PJ. Oscillatory body sway following support surface transitions: a reflection of adapting sensory gain in postural control. *Assoc Res Otolaryngol Abstr*: 234, 2002.

PROCHAZKA A. Sensorimotor gain control: a basic strategy of motor systems? *Prog Neurobiol* 33: 281–307, 1989.

SCHÖNER G. Dynamic theory of action-perception patterns: the "moving room" paradigm. *Biol Cybern* 64: 455–462, 1991.

TALBOTT RE. Postural reactions of dogs to sinusoidal motion in the peripheral visual field. *Am J Physiol Regulatory Integrative Comp Physiol* 239: R71–R79, 1980.

VAN ASTEN WNJC, GIELEN CCAM, AND DENIER VAN DER GON JJ. Postural adjustments induced by simulated motion of differently structured environments. *Exp Brain Res* 73: 371–383, 1988a.

VAN ASTEN WNJC, GIELEN CCAM, AND VAN DER GON JJ. Postural movements induced by rotations of visual scenes. *J Opt Soc Am* 5: 1781–1789, 1988b.

VAN DER KOOIJ H, JACOBS R, KOOPMAN B, AND GROOTENBOER H. A multisensory integration model of human stance control. *Biol Cybern* 80: 299–308, 1999.

VAN DER KOOIJ H, JACOBS R, KOOPMAN B, AND VAN DER HELM F. An adaptive model of sensory integration in a dynamic environment applied to human stance control. *Biol Cybern* 84: 103–115, 2001.

WATSON SR AND COLEBATCH JG. EMG responses in the soleus muscles evoked by unipolar galvanic vestibular stimulation. *Electroencephalogr Clin Neurophysiol* 105: 476–483, 1997.

WINTER DA. *Biomechanics and Motor Control of Human Movement*. New York: Wiley, 1990.

WINTER DA, PATLA AE, PRINCE F, ISHAC M, AND GIELO-PERCZAK K. Stiffness control of balance in quiet standing. *J Neurophysiol* 80: 1211–1221, 1998.

WINTER DA, PATLA AE, RIETDYK S, AND ISHAC MG. Ankle muscle stiffness in the control of balance during quiet standing. *J Neurophysiol* 85: 2630–2633, 2001.

ZAJAC FE. Muscle and tendon properties, models, scaling, and application to biomechanics and motor control. In: *Critical Reviews in Biomedical Engineering*, edited by Bourne JR. Boca Raton, FL: CRC, 1989, p. 359–411.

ZUPAN L, MERFELD DM, AND DARLOT C. Using sensory weighting to model the influence of canal, otolith and visual cues on spatial orientation and eye movements. *Biol Cybern* 86: 209–230, 2002.